Rigidity-induced critical points

Y. Grabovsky [1] and L. Truskinovsky [2]
[1]*Department of Mathematics, Temple University, Philadelphia, Pennsylvania 19122, USA*
[2]*PMMH, CNRS-UMR 7636, ESPCI, PSL, 75005 Paris, France*

(Received 14 April 2024; accepted 8 November 2024; published 9 December 2024)

While classical theory of phase transitions deals with systems in which shape variation is energetically neutral, the account of *rigidity* can lead to the emergence of new thermodynamic features. One of them is a special type of critical points that are characteristic of phase transitions specifically in solids. We develop a general theory of such rigidity-induced critical points and illustrate the results by analyzing in detail the case of an isotropic, geometrically nonlinear solid undergoing a volumetric phase transition at zero temperature.

DOI: 10.1103/PhysRevE.110.064114

I. INTRODUCTION

The conventional thermodynamic approach to phase stability of solids is to treat them mechanically as liquids. This classical perspective has been challenged by the appearance of "kinetic" or "coherent" phase diagrams for diffusionless phase transitions [1–10] and the attempts to understand the ensuing complex multiphase microstructures dominated by elastic interactions [11,12]. To corroborate the idea that the account of rigidity in solid-solid transformations can lead to fundamentally new thermodynamic effects, we focus in this paper on the emergence in elastically compatible systems of a peculiar type of critical points that do not exist in rigidity-free (liquid) systems.

A. Motivation: Swelling transition in gels

A particularly striking example of the failure of the "liquid" perspective on phase equilibria was provided by experimental studies of polymeric gels exhibiting swelling phase transition [13–16]. The presence of solvent suggests that such gels should be treated as binary mixtures with a nonconvex free-energy dependence on solvent concentration. However, the classical "liquid" picture of the implied phase separation is complicated by the presence of nonzero shear rigidity generated by cross-linking of a polymer network inside a solvent, and several peculiar "solid" features were observed during the transition between the swollen and shrunken phases [17–21]. All this pointed toward the importance of treating such gels as solids whose elastic energy is nonconvex due to enslavement of solvent concentration to the volumetric deformation of the network [21].

More specifically, in contradiction with the classical thermodynamics of symmetry-preserving isotropic-to-isotropic purely "liquid" phase transitions [16,22], experiments have shown that a discontinuous swelling of a gel can generate inhomogeneous patterns of anisotropically stressed coexisting phases. In particular, experiments pointed toward the formation of microstructures which are neither isotropic nor homogeneous with developing patterns that do not resemble the ones controlled by liquid surface tension [23–25]. Moreover, the implied domain microstructures were observed in the range of parameters where, according to the "liquid" approach, they should have been mechanically unstable [23–26]. Independently, experiments showed the possibility of small, negative values of the compressibility which, as an equilibrium effect, is a feature of nonzero rigidity. This, together with the fact that critical fluctuations in swelling gels are not seen at zero bulk modulus, as purely liquid thermodynamics would have predicted, suggests that gels cannot be adequately modeled by conventional thermodynamic theory [26,27].

In the context of the transition between swollen and deswollen gels, the "nonliquid" effects have been previously linked to long-range interactions pointing toward mean-field type description [28,29]. It was also shown that due to rigidity-induced nonlocality, mediated by transverse phonons, gels can be stabilized at negative values of the compressibility in the presence of sufficiently strong boundary constraints. It was similarly argued that the specificity of swelling phase transitions in gels is due to the absence of characteristic length in elasticity theory [30], which ensures that the activation energy of nucleation in the bulk is proportional to the volume and is therefore macroscopic, in contrast to what is usually postulated in classical thermodynamic theory [16,25].

Building upon these insights, we intend to shed additional light on why the rigidity of gels and similar soft solids has such a profound effect on their equilibrium thermodynamics. In particular, we will be concerned with the fact that in swelling gels, the observations of critical opalescence remain controversial, since the expected "liquid" scaling response has not been observed at critical points, given that they are interpreted in the framework of classical thermodynamics [16,23,31].

B. Coherency constraint

The crucial reason for developing a purely "solid" perspective on diffusionless transformations in swelling gels is that polymer networks apparently do not change their connectivity during swelling transitions. More generally, one can say that behind the nonzero value of shear modulus in polymer gels is the immutable network topology, and that it is the presence

of an implied topological constraint that enables gels to resist elastic distortions. Therefore, the observed deformations should be viewed as elastically "coherent" in the sense that the underlying macroscopic displacement fields are continuous and the associated deformation gradients are geometrically compatible in the sense of Hadamard [32–39].

To abstract this idea, the "coherent" thermodynamics views a solid as always equipped with a fixed reference state [40–48]. Such an assumption is not straightforward since in principle atoms can exchange their positions, which excludes the possibility of a nonlocal coherency constraint and implies that the equilibrium value of the shear modulus must be zero [42,49]. The emergence of rigidity is therefore ultimately associated with inherently long-living metastability [47].

In contrast, the classical nonlinear elasticity theory, e.g., Refs. [50–55], ignores the metastability aspect of elastic equilibrium and views solids as never losing topological memory about their local environments. In other words, it postulates the existence of a topologically constrained configuration space which, in particular, prohibits the mutual exchanges of atomic positions [40,46–48]. While such a constraint is just an approximation, at small temperatures the flow of defects, which is supposed to relax the internal stresses, is anomalously slow because the associated effective viscosity diverges at vanishing shear stress with an essential singularity [49,56]. Therefore, in normal conditions the "kinetic" phase diagrams, accounting for "metastable" rigidity, are usually fully adequate [57,58].

The presence of the configurational constraint, requiring that a unique reference state exists, opens a possibility for a configuration of a loaded solid body to be nontrivial at equilibrium. Suppose that $\boldsymbol{x}$ is the position of a material point in the reference state, and $\boldsymbol{y}(\boldsymbol{x})$ is its position in the deformed state. The fundamental assumption of the theory of elasticity is that the total energy can be written as an integral over the region occupied by the body in the reference configuration with the macroscopic stored-energy density function W depending only on the deformation gradient

$$\boldsymbol{F} = \nabla \boldsymbol{y}. \tag{1}$$

This assumption implies that at zero temperature the deformed equilibrium state can be found by minimizing the total energy

$$\min_{\boldsymbol{y}(\boldsymbol{x})} \int W(\boldsymbol{F}) d\boldsymbol{x}, \tag{2}$$

subject to boundary conditions that, in the case of hard device type loading, would involve restrictions on the boundary values of $\boldsymbol{y}(\boldsymbol{x})$ [50,52,59–61]. The complexity of the problem (2) is due to the fact that the tensorial argument of the function W, which plays the role of an order parameter, is a gradient of a continuous function. Therefore, the deformation gradient $\boldsymbol{F}$ at different points cannot be varied independently [42], and in addition to the Euler-Lagrange equations

$$\nabla \cdot \boldsymbol{P} = 0, \tag{3}$$

where $P_i^\alpha = \frac{\partial W}{\partial F_\alpha^i}(\boldsymbol{F})$ is the Piola stress tensor, it must satisfy a nonlocal coherency constraint

$$\operatorname{curl} \boldsymbol{F} = 0. \tag{4}$$

The latter, however, is only relevant in the presence of rigidity, as for liquids the constraint (4) is inactive and the effective locality of the minimization problem is recovered. It is also clear that, in the case of generic loading, the solutions of (2), satisfying (3) and (4), may be highly inhomogeneous.

Under the assumption of either long-living metastable configurations or internally constrained equilibrium, it is meaningful to develop the "coherent" thermodynamics of solid-solid phase transitions, which now counts many important contributions, e.g., Refs. [11,62–64]. This and other related work has already identified some generic thermodynamic anomalies associated with elastic phase transitions by linking them to long-range elastic interactions induced by the coherency constraint (4); see, for instance, Refs. [11,28,29,65]. In particular, it was understood that in systems with nonzero rigidity, the energy of phase mixtures depends not only on the volume fractions but also on the detailed microstructure of coexisting phases including both the shape and the orientation of the single phase domains [12,66,67].

Moreover, it was shown that if the bottoms of the energy wells are not geometrically compatible, in the sense that the corresponding values of $\boldsymbol{F}$ are not rank-1-connected, mixing would have an extensive energy cost [68,69]. An important resulting effect is the nonlinearity of the dependence of the elastic energy on the volume fractions of the phases in coherent multiphase mixtures [66,67]. The implied nonadditivity of the energy is also behind the macroscopic energy barrier for phase nucleation, which is ultimately responsible for metastability and rate-independent hysteresis accompanying coherent transformations [69,70]. All this invalidates the use of the common tangent (Maxwell) construction for determining phase equilibria [1,2,62,71,72], replacing the usual convexification of the energy with a more subtle construction known as quasiconvexification [60,61,73–75].

In the case of gels undergoing swelling phase transitions, the above effects can be expected to be manifestly present. Thus, since in the case of volumetric transitions the bottoms of the energy wells are not geometrically compatible, the two-phase polymer network must deform inhomogeneously. Also, the observations of negative compressibility at such transitions in a range of parameters are supported by the fact that in sufficiently constraining loading conditions, the elastic instability, associated with volumetric phase transitions, takes place strictly after the convexity of the energy has already been violated [76,77]. We emphasize that the case of volumetric phase transitions in isotropic gels is just an example, that is at the same time highly nontrivial and exactly solvable, while permitting faithful graphical representation of our results. Our general methodology, however, is applicable to arbitrary, not only volumetric, phase transitions, without any constraints on the symmetry of the coexisting phases.

C. Organization of the paper

One of the most important signature of "coherent" thermodynamics is that the tensorial stress becomes a parameter on phase diagrams replacing the conventional liquid pressure [62–64,78]. Our goal is to corroborate the idea that such an extension of the parameter space produces new

qualitative effects. In particular, we intend to show that in isotropic solids, in addition to the classical "liquid" critical points associated with volumetric phase transitions, one can also expect the emergence of specific, zero-temperature, rigidity-induced purely "solid-type" critical points.

Critical points in the configurational space can be anticipated if there is no distinction between the transforming phases in terms of their symmetry as they can be in principle continuously deformed one into another. To illustrate this general idea, we study in this paper as an example a class of phase transformations between isotropic solid phases characterized by different reference densities. The phases are supposed to be subjected to homogeneous (affine) deformations applied on the boundary. In the course of such a loading program, the deformation gradient $\boldsymbol{F}$ is expected to cross into the coherent binodal region [77,79], where the system loses stability against strong perturbations, i.e., the infinitesimal perturbations of the deformation $\boldsymbol{y}(\boldsymbol{x})$ itself that are not infinitesimal as far as the deformation gradient $\nabla\boldsymbol{y}(\boldsymbol{x})$ is concerned. The boundary of the coherent binodal region (also known as a *coherent binodal*) is then a set in the phase space of tensors $\boldsymbol{F}$ consisting of points where the energy density and its quasiconvex envelope separate [77,79–81]. This makes the corresponding homogeneous configurations marginally stable, while announcing the formation of an inhomogeneous energy-minimizing microstructure immediately upon crossing the coherent binodal. In typical cases, the coherent binodal region can be expected to separate two (or more) connected components of the phase space, which can then be identified as phases. This is the case, for instance, for liquids where the energy density W depends only on the specific volume $\det(\boldsymbol{F})$. However, when rigidity is different from zero, the stable part of the phase space can form a connected set cutting through the domain of phase coexistence and permitting passage from one phase to the other without any sharp transition and, consequently, without the concomitant microstructure development.

In such cases, one can define coherent critical points as the common limit of the two coexisting deformation gradients in two-phase equilibria, i.e., points at which distinction between the two phases in equilibrium disappears. The emergence of such points corresponds to the limiting case when the range of phase coexistence and the attendant microstructure development can shrink to a point. As in the case of P-V diagrams for liquid phase transitions, in such critical points, coherent binodals and coherent spinodals in the space of deformation gradients $\boldsymbol{F}$ are tangent to each other, which paves the way toward analytical characterization of coherent critical points. Here by *coherent spinodal* we designate the boundary of elastic stability against local weak perturbations, i.e., infinitesimally small perturbations of the deformation gradient localized in an infinitesimal neighborhood of a material point [77,82,83].

The goal of this paper is to elucidate these ideas, support them by explicit analytical computations, and then illustrate them through a systematic development of an example directly applicable to the description of swelling phase transitions in gels.

We begin the paper in Sec. II by recalling various mechanical aspects of the classical first-order symmetry-preserving phase transition in a van der Waals–type liquid phase. While the analysis is performed using nonlinear elasticity theory, it is assumed that in equilibrium all nonhydrostatic stresses relax and the elastic response can be fully represented by the pressure-density relation. In the case of interest, the system is below the classical liquid criticality; moreover, for simplicity, we assume that the temperature is equal to zero. Under these conditions, we determine the domain of equilibrium phase coexistence that is bounded by the classical thermodynamic binodal; we also determine the location of the classical thermodynamic spinodal and show that the two neither touch nor intersect. We then compute the equilibrium energy parametrized by the specific volume that describes the ground state. Expectedly, in this context, the nonclassical coherent critical points do not appear.

After reviewing these classical results, we present in Sec. III a parallel analysis for the model of a generic diffusionless phase transition in a nonlinear elastic solid, exhibiting general rigidity and allowing for arbitrary transformation strain. In this way, we permit the structure of the binodal to change qualitatively *vis à vis* the case of an elastic liquid, and pave the way toward the possibility of nonclassical, rigidity-induced critical points. We develop a general theory of such critical points in "coherent" thermodynamics, linking them to the conditions where the two coexisting phases coincide. We show that since the corresponding critical states must lie on both the spinodal and the binodal, these two surfaces in the tensorial space of deformation gradients $\boldsymbol{F}$ must be tangent at the critical points. The latter circumstance allows us to obtain an explicit analytic characterization of such critical points. The general results obtained in this section can be expected to have important implications for the design of phase equilibria in highly deformable soft condensed matter, as well as in artificial metamaterials, undergoing geometric phase transitions. Our approach avoids conventional linearization of elastic stresses and strains and is developed in the geometrically exact framework of nonlinear elasticity theory.

To illustrate these general results, we consider, in Secs. IV and V, two explicit examples showing that even in the presence of rigidity, depending on a subtle difference in material model, coherent critical points in the stress space may or may not appear.

The first example presented in Sec. IV is directly related to the swelling phase transition in gels. We consider in full detail an isotropic solid, exhibiting the simplest symmetry-preserving phase transition, with phases differing only by their specific volume. Such a transformation in liquids is known to exhibit a classical critical point in the pressure-temperature space. In this section, we show that an account of rigidity can give rise to a whole family of nonclassical critical points in the stress space. More specifically, we use the Hadamard-Flory model and show that if the elastic shear modulus is sufficiently large, one can construct a loading protocol that brings phases with different reference-specific volumes into each other continuously while passing around a rigidity-induced set of critical points. We locate this set in both stress and strain spaces, while retrieving, along the way, a nontrivial "coherent" generalization of the common tangent construction, which gives rise to nonconvex ground-state energy.

Our second example, presented in Sec. V, reveals the perils of geometrical linearization in coherent thermodynamics. We

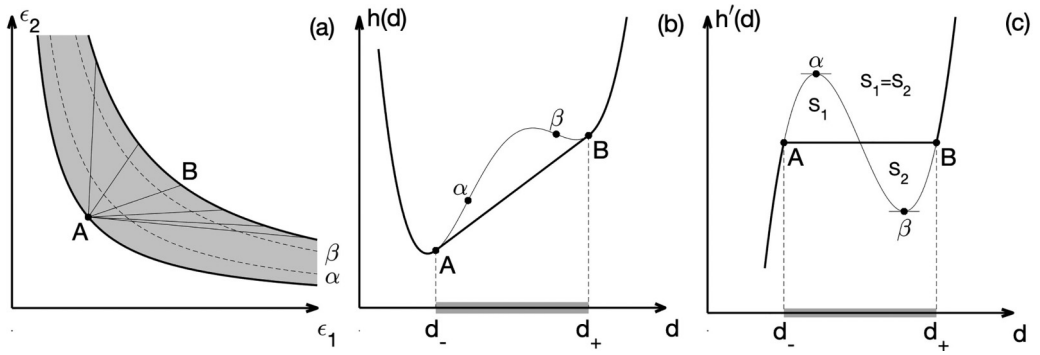

FIG. 1. Phase diagram in the space of principal strains ϵ_1 and ϵ_2 (a), double-well energy (b), and pressure-volume relation (c) for an elastic liquid. The relaxed (ground-state) energy and the relaxed stress-strain response are shown in (b) and (c) by thick solid lines. Binodal region in (a) is shaded; dashed lines limit the spinodal region. Here A and B mark coexisting states on the binodal, while α and β indicate spinodal points; dashed lines α, β in (a) enclose the spinodal region.

show that if the geometrically nonlinear model of an isotropic two-phase solid, discussed above, is replaced by the more conventional geometrically linearized description, the solid-specific critical points disappear. This example highlights the crucial importance of using geometrically exact theories of elasticity in the study of coherent phase equilibria in soft solids. It can then be viewed as a cautionary tale that geometric linearization can create unphysical artifacts in soft condensed matter.

Finally, in Sec. VI we summarize our results and present general conclusions.

II. ELASTIC FLUID

To set the stage, we first assume that the rigidity can be neglected and that the energy density of our "elastic liquid" is a function of the normalized specific volume $d = \det(\boldsymbol{F})$ only,

$$W(\boldsymbol{F}) = h(d). \tag{5}$$

Since we deal with a volumetric phase transition, the function $h(d)$ is assumed to have a double-well structure; see Fig. 1(b). This makes the hydrostatic stress (negative of the pressure) $h'(d)$ a nonmonotone up-down-up function; see Fig. 1(c). Here and in what follows, a prime denotes differentiation.

A. Classical binodal

In such an "elastic liquid" setting, the conditions of phase equilibrium are well known [84,85]. The first condition,

$$[\![h'(d)]\!] = 0, \tag{6}$$

where $[\![A]\!] = A_+ - A_-$ denotes the jump, establishes the equality of pressures in the two phases. The second,

$$[\![h(d)]\!] - h'_{\pm}(d)[\![d]\!] = 0, \tag{7}$$

known as Maxwell equal area construction, states that the chemical potentials in the two phases must be equal. In the context of calculus of variations, the Gibbs-Maxwell conditions (6) and (7) are known as Weierstrasss-Erdmann conditions on broken extremals [98]; the same conditions naturally reappear in the theory of phase transitions in elastic bars [86]. In accordance with (6) and (7), phase equilibrium takes place at a single (binodal) value of pressure.

While the above analysis is fully three-dimensional, to illustrate the structure of the elastic binodal graphically in the *strain space*, it is convenient to use the two-dimensional (2D) version of our model; see Fig. 1(a). In view of isotropy and frame indifference, the relevant strain space is a plane with the axes representing singular values of $\boldsymbol{F}$ (principal strains), which we denote $\epsilon_{1,2}$ in our 2D illustrations. The domain of phase coexistence (the binodal region) in this plane is shaded in Fig. 1(a), where the hydrostatic (spherical) deformations correspond to the line $\epsilon_1 = \epsilon_2 = \epsilon$. Note that the elastic liquid model does not allow us to specify the corresponding two phase microstructures uniquely, and, to stress this point, we indicated in Fig. 1(a) multiple admissible connections between a state A and different states B.

B. Ground-state energy

If we denote the specific volumes of the two coexisting phases $d_- \leqslant d_+$, then the relaxed (ground-state) energy density $\tilde{W}(d)$ is a convexification of $h(d)$, which at $d_- \leqslant d \leqslant d_+$, i.e., where $h(d)$ differs from its convex hull, takes the form

$$\tilde{W}(d) = \frac{d - d_-}{d_+ - d_-} h(d_+) + \frac{d_+ - d}{d_+ - d_-} h(d_-).$$

Instead, at $d \leqslant d_-$ and $d \geqslant d_+$ we have simply

$$\tilde{W}(d) = h(d).$$

The relaxed energy is shown by a thick solid line in Fig. 1(b). The corresponding equilibrium pressure-volume response is shown in Fig. 1(c), also by a thick solid line; note that the Maxwell equal area construction is operative in this case.

C. Classical spinodal

The two spinodal points in the "elastic liquid" model, d_α and d_β, are defined by the thermodynamic condition [84]

$$h''(d) = 0. \tag{8}$$

They are located inside the binodal region (between points A and B) and are explicitly indicated in Figs. 1(a)–1(c) by the letters α and β.

D. Classical critical point

We adopt, as an operational definition, that at the critical points the spinodal and the binodal meet, and therefore touch;

note that under such an assumption, a critical point is a point on the spinodal, which is stable. In liquid systems the critical points are defined by two equations. One of them is Eq. (8) because critical points belong to the spinodal. The second equation, indicating the point of tangency of the spinodal and the binodal, is [84]

$$h'''(d) = 0. \tag{9}$$

It is easy to see that the critical state $d = d_*$, which satisfies (8) and (9), can also be defined as a configuration where the distinction between the two coexisting phases, characterized by d_+ and d_- in Figs. 1(b) and 1(c), disappears.

In our (zero-temperature) "elastic liquid" model, the two conditions (8) and (9) cannot be satisfied simultaneously for a generic $h(d)$, and therefore there are no conventional thermodynamic critical points in Fig. 1(a). Equations (8) and (9) can both be satisfied if we add temperature as a parameter. Then the inconsistency between (8) and (9) can be overcome given that the increase of temperature is engineered to move the two wells of the energy density $h(d)$ toward each other. Then the value of the temperature, where the two energy wells coalesce, and therefore the two Eqs. (8) and (9) have a common solution, would correspond to a conventional thermodynamic critical point. We reiterate that our choice of zero temperature is made to ensure that the classical critical points are taken out of the picture, so that we could fully focus on the novel nonclassical critical points.

To find where any distinction between solid phases, coexisting in equilibrium, disappears, we need to generalize the equilibrium conditions (6), (7), (8), and (9) for the case of general elastic solids. While the analogs of the first three are basically known, the fully tensorial counterpart of (9) is not, and it would have to be derived here.

III. ELASTIC SOLID

In this section, we consider an elastic solid with nonzero rigidity, and we use the methods of "coherent" thermodynamics to locate the coherent binodal and spinodal in the strain space. As a by-product, we also identify the location of the rigidity-induced critical points. In physical terms, the general class of solids considered in this section can be characterized as proper displacive with elastic strain playing the role of order parameter [87–90]. In this sense, the swelling transition in gels can also be interpreted as displacive with coexisting phases differing by density and, therefore, linked only by a trivial symmetry transformation.

A. Coherent binodal

The "coherent" analogs of conventional thermodynamic (liquid) equilibrium conditions (6) and (7) can also be viewed as equations that the *coexisting* deformation gradients $\boldsymbol{F}_\pm$ must satisfy. Here it is implied that a continuous, piecewise affine deformation $\boldsymbol{y}_\pm(\boldsymbol{x})$, characterized by the two gradients $\nabla \boldsymbol{y}_\pm(\boldsymbol{x}) = \boldsymbol{F}_\pm$, which are separated by a plane of discontinuity of the deformation gradients, is elastically stable.

To derive the corresponding conditions, we start with the reminder that the relevant consequence of the elastic stability of the homogeneous configuration $\boldsymbol{y}(\boldsymbol{x}) = \boldsymbol{F}\boldsymbol{x}$ with respect to all perturbations $\widetilde{\boldsymbol{y}}$ that agree with $\boldsymbol{y}(\boldsymbol{x})$ on the boundary and are uniformly close to $\boldsymbol{y}(\boldsymbol{x})$ is the Weierstrass condition [73,91,92],

$$W(\boldsymbol{F} + \boldsymbol{a} \otimes \boldsymbol{n}) \geqslant W(\boldsymbol{F}) + W_{\boldsymbol{F}}(\boldsymbol{F})\boldsymbol{n} \cdot \boldsymbol{a} \tag{10}$$

for all vectors $\boldsymbol{a}$ and $|\boldsymbol{n}| = 1$; here and in what follows, the *tensorial* subscripts indicate partial differentiation with respect to the components of the corresponding tensorial variables. In physical terms, condition (10) expresses stability of the homogeneous configuration with respect to *nucleation* of coherent lamina of the new phase [74,93]. Here $\boldsymbol{n}$ is the normal to the layers of the nucleating laminate in Lagrangian coordinates, and $\boldsymbol{a}$ is the shear (polarization) vector, indicating the additional shear that, say, an image of the vector $\boldsymbol{n}$ in the deformed configuration undergoes as a result of the transformation. The "liquid" analog of (10) is the condition of convexity of the function $h(d)$ from (5) at the point d.

Geometrically, inequality (10) partitions the space of deformation gradients $\boldsymbol{F}$ into two regions: the region $\mathcal{B}_{\mathcal{W}}$, where the Weierstrass necessary condition (10) fails, all of whose points are definitively unstable, and its complement. While each point $\boldsymbol{F}$ in the complement of $\mathcal{B}_{\mathcal{W}}$ satisfies (10), it does not guarantee its stability, i.e., quasiconvexity of $W(\boldsymbol{F})$. We will call the surface $\partial\mathcal{B}_{\mathcal{W}}$ the *Weierstrass binodal*. Since (10) is only a necessary but not a sufficient condition of elastic stability, the region $\mathcal{B}_{\mathcal{W}}$ lies inside the coherent binodal region $\mathcal{B}$. The latter comprises the set of all elastically unstable homogeneous (affine) configurations. Therefore, all stable points on the Weierstrass binodal must necessarily lie on the coherent binodal $\partial\mathcal{B}$. The notion of (coherent) binodal was introduced in [77,80], where it was also explained why such a binodal marks the boundary of quasiconvexity of the energy density.

While the simple constructive characterization of the coherent binodal is hardly possible, the Weierstrass binodal is relatively easy to describe algebraically. Its equations can be found by regarding inequality (10) as the requirement that the pairs $(\boldsymbol{a}, \boldsymbol{n}) = (0, \boldsymbol{n})$, where $\boldsymbol{n}$ is an arbitrary unit vector, are *absolute* minimizers of

$$\Delta(\boldsymbol{a}, \boldsymbol{n}) = W(\boldsymbol{F} + \boldsymbol{a} \otimes \boldsymbol{n}) - W_{\boldsymbol{F}}(\boldsymbol{F})\boldsymbol{n} \cdot \boldsymbol{a}. \tag{11}$$

Indeed, when $\boldsymbol{F} \in \mathcal{B}_{\mathcal{W}}$, and this condition fails, there exist $\boldsymbol{a} \neq 0$ and $|\boldsymbol{n}| = 1$ for which $\Delta(\boldsymbol{a}, \boldsymbol{n}) < W(\boldsymbol{F})$.

Note next that on the Weierstrass binodal $\partial\mathcal{B}_{\mathcal{W}}$ we expect the existence of $(\boldsymbol{a}, \boldsymbol{n})$, such that $\Delta(\boldsymbol{a}, \boldsymbol{n}) = W(\boldsymbol{F})$, with $(\boldsymbol{a}, \boldsymbol{n})$ being a global minimizer of Δ. Then, for all $\boldsymbol{F} \in \partial\mathcal{B}_{\mathcal{W}}$ the following necessary conditions must hold:

$$\Delta_{\boldsymbol{a}}(\boldsymbol{a}, \boldsymbol{n}) = 0, \tag{12}$$

$$\Delta_{\boldsymbol{n}}(\boldsymbol{a}, \boldsymbol{n}) = 0, \tag{13}$$

$$\Delta(\boldsymbol{a}, \boldsymbol{n}) = W(\boldsymbol{F}). \tag{14}$$

Introducing the notation $\boldsymbol{F}_- = \boldsymbol{F}$, $\boldsymbol{F}_+ = \boldsymbol{F} + \boldsymbol{a} \otimes \boldsymbol{n}$, which ensures that $\boldsymbol{F}_-$ and $\boldsymbol{F}_+$ are values of the gradient of a *continuous* displacement field, we obtain the Hadamard kinematic compatibility condition [50,52,59–61],

$$[\![\boldsymbol{F}]\!] = \boldsymbol{a} \otimes \boldsymbol{n}, \tag{15}$$

where $\boldsymbol{a}$ is the shear vector, and $\boldsymbol{n}$ is the unit normal to the phase boundary; this condition has often appeared under

different names; see, for instance, the "nondisruption condition" in [94] and the condition on "domain-wall orientations" in [95]. We can then rewrite Eqs. (12)–(14) in the form of a system

$$[\![\boldsymbol{P}]\!]\boldsymbol{n} = 0, \tag{16}$$

$$[\![\boldsymbol{P}]\!]^T\boldsymbol{a} = 0, \tag{17}$$

$$[\![W]\!] - \boldsymbol{P}_\pm\boldsymbol{n}\cdot\boldsymbol{a} \equiv [\![W]\!] - \{\boldsymbol{P}\}\boldsymbol{n}\cdot\boldsymbol{a} = 0, \tag{18}$$

where $\boldsymbol{P}_\pm = W_{\boldsymbol{F}}(\boldsymbol{F}_\pm)$ and $\{A\} = (1/2)(A_+ + A_-)$.

The first Eq. (16) in this system is the classical traction continuity condition [50,61]. The last Eq. (18) is a generalization of the Maxwell equilibrium condition [96]; the analogs of both of these conditions are already present in the theory of fluid equilibria; see (6) and (7).

Note that the conditions (16) and (18) can also be viewed as tensorial analogs of the classical Weierstrass-Erdmann conditions on broken extremals [97–101]. They are well known in the calculus of variations and have also been used extensively in coherent thermodynamics of elastic phase transitions [12,60,102–110].

Instead, condition (17) is *solid-specific* and, in this sense, rigidity-induced, as it does not exist in classical thermodynamics of liquid phases. Not being relevant in the simplest scalar problem studied by Weierstrass, it has also been overlooked for a long time in the context of calculus of variations. While the necessity of additional equalities on smooth broken extremals has been felt for a long time [106,111–117], in the present general form condition (17) was first obtained only recently [80]. As follows from its derivation, see Eq. (13), the condition (17) emerges from testing the equilibrium phase coexistence against local reorientations of the phase boundary viewed as a surface of discontinuity of the deformation gradients; see [81] for further details.

The complete system of Eqs. (15)–(18) describes a *jump set*, a hypersurface (surface of codimension 1) in the phase space (space of deformation gradients $\boldsymbol{F}$) which contains the Weierstrass binodal $\partial\mathcal{B}_{\mathcal{W}}$, but may also contain branches that lie inside $\mathcal{B}_{\mathcal{W}}$. In this sense, the Weierstrass binodal delineates the outer envelope of the *jump set*, stable parts of which belong to the coherent binodal. By emphasizing this point, we stress that, while it is never an issue in liquid systems, some of the ensuing thermodynamic phase equilibria can still be elastically unstable.

One way to distinguish stable points on $\partial\mathcal{B}_{\mathcal{W}}$ from those inside $\mathcal{B}_{\mathcal{W}}$ is to check the non-negativity of the Hessian

$$\boldsymbol{H} = \begin{bmatrix} \Delta_{aa} & \Delta_{an} \\ \Delta_{na} & \Delta_{nn} \end{bmatrix}.$$

It turns out that on the part of the hypersurface (15)–(18) that satisfies $\boldsymbol{H} > 0$, each $\boldsymbol{F} = \boldsymbol{F}_-$ has a uniquely defined $\boldsymbol{F}_+$ that depends smoothly on $\boldsymbol{F}_-$. Note that the positive definiteness of $\boldsymbol{H}$ has to be understood, while accounting for its geometrical degeneracy induced by the fact that the Weierstrass condition depends on $\boldsymbol{a}$ and $\boldsymbol{n}$ only through the combination $\boldsymbol{a}\otimes\boldsymbol{n}$.

In what follows, we denote by $\mathcal{J}$ the part of the hypersurface (15)–(18) that satisfies $\boldsymbol{H} > 0$. In our example of Hadamard-Flory solid, discussed in Sec. IV, the whole hypersurface defined by (15)–(18) will have this property. It will also coincide with the coherent binodal. In our geometrically linear example considered in Sec. V, the surface defined by (15)–(18) also coincides with the coherent binodal, but it has $\boldsymbol{H} = 0$ at each point. As we are going to see, the degeneracy is, in part, due to the enhanced compatibility of the linearized strain.

B. Coherent spinodal

One of the elementary consequences of the Weierstrass stability condition (10) is obtained by restricting $\boldsymbol{a}$ to a small neighborhood of zero. From the expansion

$$W(\boldsymbol{F}+\boldsymbol{a}\otimes\boldsymbol{n}) - W(\boldsymbol{F}) - W_{\boldsymbol{F}}(\boldsymbol{F})\boldsymbol{n}\cdot\boldsymbol{a} = \frac{1}{2}\boldsymbol{A}(\boldsymbol{F};\boldsymbol{n})\boldsymbol{a}\cdot\boldsymbol{a} + O(|\boldsymbol{a}|^3),$$

we obtain a corollary of (10), known as the Legendre-Hadamard condition, or the ellipticity condition for equations of elastostatics, e.g. [60,61,118],

$$\boldsymbol{A}(\boldsymbol{F};\boldsymbol{n})\boldsymbol{a}\cdot\boldsymbol{a} \geqslant 0, \tag{19}$$

for all $|\boldsymbol{a}| = 1$ and $|\boldsymbol{n}| = 1$. Here $\boldsymbol{A}(\boldsymbol{F};\boldsymbol{n})$ is the acoustic tensor defined by its quadratic form

$$\boldsymbol{A}(\boldsymbol{F};\boldsymbol{n})\boldsymbol{a}\cdot\boldsymbol{a} = W_{\boldsymbol{FF}}(\boldsymbol{F})[\boldsymbol{a}\otimes\boldsymbol{n}, \boldsymbol{a}\otimes\boldsymbol{n}],$$

or in index notation, by the formula

$$A_{ij}(\boldsymbol{F};\boldsymbol{n}) = W_{F^i_\alpha F^j_\beta}(\boldsymbol{F})n_\alpha n_\beta,$$

where the summation over repeated indexes is assumed.

Just as in the case of the Weierstrass binodal, it is advantageous to view (19) geometrically as a partitioning of the phase space into two regions: $\mathcal{S}$, where (19) fails (coherent spinodal region), and its complement. The boundary $\partial\mathcal{S}$ can then be interpreted as the coherent spinodal; see [77] for further details.

According to (19), all the eigenvalues of real symmetric matrices $\boldsymbol{A}(\boldsymbol{F};\boldsymbol{n})$ have to be non-negative for all $|\boldsymbol{n}| = 1$. While the computation of eigenvalues of real symmetric matrices is standard, the verification of their non-negativity for an infinite family of unit vectors $\boldsymbol{n}$ can make the task challenging.

To overcome this difficulty, we first emphasize that when $\boldsymbol{F} \in \partial\mathcal{S}$, there exists a unit vector $\boldsymbol{n}_0$, such that at least one of the eigenvalues of the acoustic tensor $\boldsymbol{A}(\boldsymbol{F};\boldsymbol{n}_0)$ becomes zero, while others remain positive. In addition, the eigenvalues of $\boldsymbol{A}(\boldsymbol{F};\boldsymbol{n})$ must be non-negative for *all* unit vectors $\boldsymbol{n}$. Denoting by $\boldsymbol{a}_0$ the unit eigenvector of $\boldsymbol{A}(\boldsymbol{F};\boldsymbol{n}_0)$ corresponding to the zero eigenvalue, we obtain our first set of equations for the coherent spinodal,

$$\boldsymbol{A}(\boldsymbol{F};\boldsymbol{n}_0)\boldsymbol{a}_0 = 0. \tag{20}$$

The second set is obtained from the observation that $\Lambda(\boldsymbol{n}) = \boldsymbol{A}(\boldsymbol{F};\boldsymbol{n})\boldsymbol{a}_0\cdot\boldsymbol{a}_0$ achieves its global minimum of 0 at $\boldsymbol{n} = \boldsymbol{n}_0$, so that

$$\boldsymbol{A}^*(\boldsymbol{F};\boldsymbol{a}_0)\boldsymbol{n}_0 = 0, \tag{21}$$

where $\boldsymbol{A}^*(\boldsymbol{F};\boldsymbol{a})$ is the co-acoustic tensor defined by its quadratic form

$$\boldsymbol{A}^*(\boldsymbol{F};\boldsymbol{a})\boldsymbol{n}\cdot\boldsymbol{n} = W_{\boldsymbol{FF}}(\boldsymbol{F})[\boldsymbol{a}\otimes\boldsymbol{n},\boldsymbol{a}\otimes\boldsymbol{n}]$$

or in index notation by the formula

$$A^{*\alpha\beta}(\boldsymbol{F};\boldsymbol{a}) = W_{F^i_\alpha F^j_\beta}(\boldsymbol{F})a^i a^j,$$

where we again assumed the summation over repeated indexes.

Equations (20) and (21), satisfied by all points on the coherent spinodal, can be viewed as the tensorial analogs of (8). Upon elimination of the unit vectors $\boldsymbol{n}_0$ and $\boldsymbol{a}_0$, they describe a hypersurface in the phase space of deformation gradients $\boldsymbol{F}$. Indeed, in n space dimensions there are $n^2+(n-1)+(n-1)$ unknowns in the set of tensorial variables $(\boldsymbol{F},\boldsymbol{a}_0,\boldsymbol{n}_0)$, since both $\boldsymbol{a}_0$ and $\boldsymbol{n}_0$ are unit vectors. Equation (20) has n scalar restrictions, as does Eq. (21). However, there is one scalar relation between the two equations, since

$$\boldsymbol{A}^*(\boldsymbol{F};\boldsymbol{a}_0)\boldsymbol{n}_0\cdot\boldsymbol{n}_0 = \boldsymbol{A}(\boldsymbol{F};\boldsymbol{n}_0)\boldsymbol{a}_0\cdot\boldsymbol{a}_0.$$

Thus, the space of solutions $(\boldsymbol{F},\boldsymbol{a}_0,\boldsymbol{n}_0)$ of (20) and (21) is (n^2-1)-dimensional. Therefore, under some basic nondegeneracy assumptions, we can claim that the solution set has (n^2-1)-dimensional projection onto the phase space of deformation gradients $\boldsymbol{F}$. Note that while all points on the coherent spinodal solve the system (20) and (21), such a system by itself may also have other solution branches, all in the interior of $\mathcal{S}$.

C. Coherent critical points

Recall that we defined *coherent critical points* as the points of intersection, and therefore tangency, of the coherent binodal and the coherent spinodal. This operational definition implies that critical points are exactly the stable points on the spinodal, in particular, the corresponding states (deformation gradients $\boldsymbol{F}_*$) must satisfy the necessary condition of Weierstrass (10).

Using $\boldsymbol{a}=t\boldsymbol{a}_0$ and $\boldsymbol{n}=\boldsymbol{n}_0$ in the Weierstrass condition (10), we obtain

$$\begin{aligned} &W(\boldsymbol{F}_*+t\boldsymbol{a}_0\otimes\boldsymbol{n}_0) - W(\boldsymbol{F}_*) - tW_{\boldsymbol{F}}(\boldsymbol{F})\boldsymbol{n}_0\cdot\boldsymbol{a}_0 \\ &\quad = \frac{t^3}{6}W_{\boldsymbol{FFF}}(\boldsymbol{F}_*)[\boldsymbol{a}_0\otimes\boldsymbol{n}_0,\boldsymbol{a}_0\otimes\boldsymbol{n}_0,\boldsymbol{a}_0\otimes\boldsymbol{n}_0]+O(t^4), \end{aligned}$$

where we used that

$$\boldsymbol{A}(\boldsymbol{F}_*;\boldsymbol{n}_0)\boldsymbol{a}_0\cdot\boldsymbol{a}_0 = 0. \tag{22}$$

Furthermore, given that the leading term above has an odd power of t, inequality (10) implies that we must have

$$W_{\boldsymbol{FFF}}(\boldsymbol{F}_*)[\boldsymbol{a}_0\otimes\boldsymbol{n}_0,\boldsymbol{a}_0\otimes\boldsymbol{n}_0,\boldsymbol{a}_0\otimes\boldsymbol{n}_0] = 0. \tag{23}$$

This equation shows that if $\boldsymbol{F}_*\in\partial\mathcal{S}$ is stable, then $\boldsymbol{F}$ must satisfy (20), (21), and (23). Upon elimination of unit vectors $\boldsymbol{a}_0$ and $\boldsymbol{n}_0$, we are left with two scalar equations, locating the state $\boldsymbol{F}_*$ on a codimension-1 subvariety of the spinodal.

Let us now demonstrate that critical points admit a more classical description as points in the phase space, where the distinction between the two coexisting phases disappears. Recall that if $\boldsymbol{F}_*$ is a point of tangency between the coherent binodal and the coherent spinodal, then it must also be a point of tangency between the Weierstrass binodal $\partial\mathcal{B}_{\mathcal{W}}$ and the coherent spinodal. Indeed, on the one hand, all points in the complement of the coherent binodal region $\mathcal{B}$ are stable, and therefore satisfy the Weierstrass necessary condition (10). On the other hand, all points in the coherent spinodal region $\mathcal{S}$ fail (10). Therefore, the Weierstrass binodal must pass between $\partial\mathcal{B}$ and $\partial\mathcal{S}$, separating $\mathcal{S}$ from the complement of $\mathcal{B}$. Hence, $\partial\mathcal{B}_{\mathcal{W}}$ must be tangent to $\partial\mathcal{S}$ at the point $\boldsymbol{F}_*$, where $\partial\mathcal{B}$ and $\partial\mathcal{S}$ touch.

Suppose $\boldsymbol{F}_-\in\partial\mathcal{B}_{\mathcal{W}}$ is an arbitrary sequence or family of points on $\partial\mathcal{B}_{\mathcal{W}}$, such that $\boldsymbol{F}_-\to\boldsymbol{F}_*$. We claim that, generically, the corresponding $\boldsymbol{F}_+$ on $\partial\mathcal{B}_{\mathcal{W}}$, solving the jump set Eqs. (15)–(18), must also satisfy $\boldsymbol{F}_+\to\boldsymbol{F}_*$. This is based on the observation that generically the failure of the pairs $(0,\boldsymbol{n})$ to be global minimizers of $\Delta(\boldsymbol{a},\boldsymbol{n})$ occurs either by $(0,\boldsymbol{n})$ failing to be a local minimizer or by the appearance of an additional global minimizer $(\boldsymbol{a},\boldsymbol{n})$, *but not both at the same time*. In this case, if $\boldsymbol{F}_+$ does not converge to $\boldsymbol{F}_*$, when $\boldsymbol{F}_-$ does, then $\boldsymbol{F}_+\to\boldsymbol{F}_*+\boldsymbol{a}\otimes\boldsymbol{n}$, for some $\boldsymbol{a}\neq 0$ and $|\boldsymbol{n}|=1$. But then, $(\boldsymbol{a},\boldsymbol{n})$ is a global minimizer of $\Delta(\boldsymbol{a},\boldsymbol{n})$, when $\boldsymbol{F}=\boldsymbol{F}_*$. It follows that as $\boldsymbol{F}_*$ moves into the spinodal region, the minimality of $\{(0,\boldsymbol{n}):|\boldsymbol{n}|=1\}$ is violated both locally and globally, which is a nongeneric behavior. We conclude that generically, if $\boldsymbol{F}_-\to\boldsymbol{F}_*$, then $\boldsymbol{F}_+\to\boldsymbol{F}_*$ as well. Thus, each critical point must also be the common limit of a family of coexisting states $\boldsymbol{F}_+$, $\boldsymbol{F}_-$, satisfying phase equilibrium Eqs. (15)–(18).

Let us show that conversely, any point $\boldsymbol{F}_*$ on the Weierstrass binodal (the jump set) at which the distinction between $\boldsymbol{F}_+$ and $\boldsymbol{F}_-$ disappears has to satisfy Eqs. (20), (21), and (23). Specifically, we assume that for an arbitrary smooth curve $\boldsymbol{F}_-(t)$ on the Weierstrass binodal, such that $\boldsymbol{F}_-(0)=\boldsymbol{F}_*$, there exists a corresponding smooth curve $\boldsymbol{F}_+(t)$, such that $\boldsymbol{F}_+(0)=\boldsymbol{F}_*$ and $\boldsymbol{F}_\pm(t)$ solve the jump set Eqs. (15)–(18) for every (sufficiently small) t. While all points $\boldsymbol{F}_\pm(t)$ are constrained by (15)–(18) when $t\neq 0$, at the critical point the system (15)–(18) trivializes, as it is automatically satisfied whenever $\boldsymbol{F}_+=\boldsymbol{F}_-$. To overcome such an obstacle, we need to "zoom in" to the neighborhood of the critical point $\boldsymbol{F}_*$ and compute the leading-order expansions of Eqs. (15)–(18) around it.

First of all, it is important to ensure that the curve $\boldsymbol{F}(t)$ has a nonsingular parametrization. The most convenient choice of the parameter would be

$$s = |\boldsymbol{F}_+(t)-\boldsymbol{F}_-(t)|,$$

where $|\boldsymbol{F}|$ denotes the Frobenius norm of a matrix $\boldsymbol{F}$, and we use the parameter s in what follows. In this case, we can write $[\![\boldsymbol{F}]\!] = s\hat{\boldsymbol{a}}(s)\otimes\boldsymbol{n}(s)$, where $|\hat{\boldsymbol{a}}(s)|=1$, and $|\boldsymbol{a}|$ denotes the usual Euclidean length of a vector $\boldsymbol{a}$. Differentiating (in s) Eq. (15), we obtain at $s=0$,

$$[\![\dot{\boldsymbol{F}}]\!] = \hat{\boldsymbol{a}}(0)\otimes\boldsymbol{n}(0).$$

Differentiating Eqs. (16) and (17), we obtain, at $s=0$, Eqs. (20) and (21), respectively, with $\boldsymbol{a}_0=\hat{\boldsymbol{a}}(0)$ and $\boldsymbol{n}_0=\boldsymbol{n}(0)$. Thus, we have shown that any point $\boldsymbol{F}_*\in\partial\mathcal{B}_{\mathcal{W}}$ at which the distinction between phases disappears must solve the system of Eqs. (20) and (21). In particular, $\boldsymbol{F}_*$ must lie in the closure of $\mathcal{S}$. Since we have seen that the Legendre-Hadamard condition (19) is a consequence of the Weierstrass

condition (10), the spinodal must necessarily lie in the closure of $\mathcal{B}$. We conclude that $\boldsymbol{F}_* \in \partial\mathcal{B}_{\mathcal{W}}$ must also lie on the spinodal $\partial\mathcal{S}$.

Let us show now that the leading term in the expansion of the remaining Eq. (18) coincides with (23). To make the calculations more compact, we introduce the "directional derivatives" notation for multiple derivatives with respect to $\boldsymbol{F}$:

$$W_{F_\alpha^i}(\boldsymbol{F})H_\alpha^i = P[\boldsymbol{H}],$$
$$W_{F_\alpha^i F_\beta^j}(\boldsymbol{F})H_\alpha^i G_\beta^j = L[\boldsymbol{G},\boldsymbol{H}],$$
$$W_{F_\alpha^i F_\beta^j F_\gamma^k}(\boldsymbol{F})H_\alpha^i G_\beta^j K_\gamma^k = M[\boldsymbol{K},\boldsymbol{G},\boldsymbol{H}],$$

where we again assumed the summation over repeated indexes. The first derivative of the Maxwell condition (18) in s would then be

$$[\![P[\dot{\boldsymbol{F}}]]\!] - L_\pm[\dot{\boldsymbol{F}}_\pm, [\![\boldsymbol{F}]\!]] - P_\pm[[\![\dot{\boldsymbol{F}}]\!]] = 0.$$

Since $\boldsymbol{F}_\pm(0) = \boldsymbol{F}_*$, the left-hand side of the equation above is zero at $s = 0$. Hence, we must take another derivative to find the leading term. Differentiating the left-hand side above, we obtain

$$[\![L[\dot{\boldsymbol{F}},\dot{\boldsymbol{F}}]]\!] + [\![P[\ddot{\boldsymbol{F}}]]\!] - M_\pm[\dot{\boldsymbol{F}}_\pm,\dot{\boldsymbol{F}}_\pm,[\![\boldsymbol{F}]\!]] - L_\pm[\ddot{\boldsymbol{F}}_\pm,[\![\boldsymbol{F}]\!]] - 2L_\pm[\dot{\boldsymbol{F}}_\pm,[\![\dot{\boldsymbol{F}}]\!]] - P_\pm[[\![\ddot{\boldsymbol{F}}]\!]] = 0.$$

Now, at $s = 0$ we obtain $L_*[[\![\dot{\boldsymbol{F}}]\!],[\![\dot{\boldsymbol{F}}]\!]] = 0$, where L_* denotes $W_{\boldsymbol{FF}}(\boldsymbol{F}_*)$. As we have already shown,

$$[\![\dot{\boldsymbol{F}}]\!] = \boldsymbol{a}_0 \otimes \boldsymbol{n}_0, \tag{24}$$

and since $\boldsymbol{F}_*, \boldsymbol{a}_0, \boldsymbol{n}_0$ satisfy (20), then

$$L_*[[\![\dot{\boldsymbol{F}}]\!],[\![\dot{\boldsymbol{F}}]\!]] = \boldsymbol{A}(\boldsymbol{F}_*;\boldsymbol{n}_0)\boldsymbol{a}_0\cdot\boldsymbol{a}_0 = 0.$$

Hence, another differentiation in s at $s = 0$ needs to be computed. This time, we will not write the expression for the third derivative of (18), but only the value at $s = 0$. After performing obvious cancellations, we obtain

$$[\![M_*[\dot{\boldsymbol{F}},\dot{\boldsymbol{F}},\dot{\boldsymbol{F}}]]\!] + 3[\![L_*[\ddot{\boldsymbol{F}},\dot{\boldsymbol{F}}]]\!] - 3M_*[\dot{\boldsymbol{F}}_\pm,\dot{\boldsymbol{F}}_\pm,[\![\dot{\boldsymbol{F}}]\!]] - 3L_*[\ddot{\boldsymbol{F}}_\pm,[\![\dot{\boldsymbol{F}}]\!]] - 3L_*[\dot{\boldsymbol{F}}_\pm,[\![\ddot{\boldsymbol{F}}]\!]] = 0.$$

Here M_* denotes $W_{\boldsymbol{FFF}}(\boldsymbol{F}_*)$. Expanding the jump notation, it is easy to check that

$$[\![L_*[\ddot{\boldsymbol{F}},\dot{\boldsymbol{F}}]]\!] - L_*[\ddot{\boldsymbol{F}}_\pm,[\![\dot{\boldsymbol{F}}]\!]] - L_*[\dot{\boldsymbol{F}}_\pm,[\![\ddot{\boldsymbol{F}}]\!]] = \mp L_*[[\![\ddot{\boldsymbol{F}}]\!],[\![\dot{\boldsymbol{F}}]\!]],$$

and similarly

$$[\![M_*[\dot{\boldsymbol{F}},\dot{\boldsymbol{F}},\dot{\boldsymbol{F}}]]\!] - 3M_*[\dot{\boldsymbol{F}}_\pm,\dot{\boldsymbol{F}}_\pm,[\![\dot{\boldsymbol{F}}]\!]] = \mp 3M_*[\dot{\boldsymbol{F}}_\pm,[\![\dot{\boldsymbol{F}}]\!],[\![\dot{\boldsymbol{F}}]\!]] + M_*[[\![\dot{\boldsymbol{F}}]\!],[\![\dot{\boldsymbol{F}}]\!],[\![\dot{\boldsymbol{F}}]\!]].$$

The third derivative of the Maxwell relation then simplifies to

$$\mp 3M_*[\dot{\boldsymbol{F}}_\pm,[\![\dot{\boldsymbol{F}}]\!],[\![\dot{\boldsymbol{F}}]\!]] + M_*[[\![\dot{\boldsymbol{F}}]\!],[\![\dot{\boldsymbol{F}}]\!],[\![\dot{\boldsymbol{F}}]\!]] \mp 3L_*[[\![\ddot{\boldsymbol{F}}]\!],[\![\dot{\boldsymbol{F}}]\!]] = 0.$$

Taking into account that

$$[\![\dot{\boldsymbol{F}}]\!] = \boldsymbol{a}_0\otimes\boldsymbol{n}_0,$$
$$[\![\ddot{\boldsymbol{F}}]\!] = 2[\hat{\boldsymbol{a}}'(0)\otimes\boldsymbol{n}_0 + \boldsymbol{a}_0\otimes\boldsymbol{n}'(0)],$$

where $\hat{\boldsymbol{a}}'(0)$ and $\boldsymbol{n}'(0)$ denote derivatives of $\hat{\boldsymbol{a}}(s)$ and $\boldsymbol{n}(s)$ at $s = 0$, we compute

$$L_*[[\![\ddot{\boldsymbol{F}}]\!],[\![\dot{\boldsymbol{F}}]\!]] = 2\boldsymbol{A}(\boldsymbol{F}_*,\boldsymbol{n}_0)\boldsymbol{a}_0\cdot\hat{\boldsymbol{a}}'(0) + 2\boldsymbol{A}^*(\boldsymbol{F}_*,\boldsymbol{a}_0)\boldsymbol{n}_0\cdot\boldsymbol{n}'(0) = 0,$$

where we used (20) and (21). We conclude that the leading term in the Maxwell relation is

$$M_*[[\![\dot{\boldsymbol{F}}]\!],[\![\dot{\boldsymbol{F}}]\!],[\![\dot{\boldsymbol{F}}]\!]] \mp 3M_*[\dot{\boldsymbol{F}}_\pm,[\![\dot{\boldsymbol{F}}]\!],[\![\dot{\boldsymbol{F}}]\!]] = 0. \tag{25}$$

Now adding both equations (one for each sign), we obtain

$$M_*[[\![\dot{\boldsymbol{F}}]\!],[\![\dot{\boldsymbol{F}}]\!],[\![\dot{\boldsymbol{F}}]\!]] = 0,$$

which, due to (24), coincides with (23), showing that the two interpretations of criticality, (i) as the points of tangency of the coherent binodal and the coherent spinodal, and (ii) as points, where the distinction between coexisting phases disappear, coincide.

Observe now that (23) is not the only consequence of (25). We also obtain

$$M_*[\dot{\boldsymbol{F}}_\pm,[\![\dot{\boldsymbol{F}}]\!],[\![\dot{\boldsymbol{F}}]\!]] = 0.$$

Since $\boldsymbol{F}_-(s)$ was an arbitrary curve on $\partial\mathcal{B}_{\mathcal{W}}$ passing through $\boldsymbol{F}_*$ at $s = 0$, the normal to the Weierstrass binodal at $\boldsymbol{F}_*$ can be identified with the functional

$$\boldsymbol{N}_* = M_*[\boldsymbol{a}_0\otimes\boldsymbol{n}_0,\boldsymbol{a}_0\otimes\boldsymbol{n}_0,\_\,] \tag{26}$$

in the sense that

$$M_*[\boldsymbol{a}_0\otimes\boldsymbol{n}_0,\boldsymbol{a}_0\otimes\boldsymbol{n}_0,\boldsymbol{T}] = 0$$

for any tangent $\boldsymbol{T}$ to the Weierstrass binodal at $\boldsymbol{F}_*$.

Next, we show that Eq. (23) is the only equation, in addition to (20) and (21), that all critical points must satisfy. At first glance, there should be many more equations, since when two generic hypersurfaces in an n-dimensional space with equations $F(\boldsymbol{x}) = 0$ and $G(\boldsymbol{x}) = 0$ touch, the equations for the point of tangency are not only the two equations above, but also $\nabla F = \lambda\nabla G$, expressing the collinearity of the normals to the two surfaces at the point of tangency. This gives an *a priori* overdetermined (since tangency of two surfaces is not a generic configuration) system of $n+2$ equations on $n+1$ unknowns $\boldsymbol{x}$, λ. This overdeterminacy is the mathematical underpinning of our claim that when $\boldsymbol{F}_- \to \boldsymbol{F}_* \in \partial\mathcal{B}_{\mathcal{W}} \cap \partial\mathcal{S}$, then, generically, $\boldsymbol{F}_+ \to \boldsymbol{F}_*$.

Therefore, in the case of the tangency of the binodal and the spinodal, we need to examine the relation between their normals at $\boldsymbol{F}_*$, in addition to the equations that place $\boldsymbol{F}_*$ on both $\partial\mathcal{S}$ and $\partial\mathcal{B}_{\mathcal{W}}$. The normal to the binodal is given by (26). Let us compute the normal to the spinodal at an arbitrary point $\boldsymbol{F}_0 \in \partial\mathcal{S}$. To this end, we consider an arbitrary smooth curve $\boldsymbol{F}(t)$ on the spinodal, such that $\boldsymbol{F}(0) = \boldsymbol{F}_0$. For each t, there are corresponding unit vectors $\boldsymbol{a}(t)$ and $\boldsymbol{n}(t)$, such that Eqs. (20) and (21) are satisfied by $\boldsymbol{F}(t)$, $\boldsymbol{a}(t)$, $\boldsymbol{n}(t)$. Assuming that the functions above are smooth, and differentiating these equations with respect to t at $t = 0$, we will obtain a single scalar linear constraint that the tangent $\dot{\boldsymbol{F}}(0)$ to the spinodal has to satisfy, thereby revealing the normal to the spinodal. To perform the differentiation, it will be convenient

to rewrite (20) and (21) in a more generic form,

$$L[\boldsymbol{a}(t)\otimes\boldsymbol{n}(t),\boldsymbol{a}(t)\otimes\boldsymbol{u}]=0, \tag{27}$$

$$L[\boldsymbol{a}(t)\otimes\boldsymbol{n}(t),\boldsymbol{v}\otimes\boldsymbol{n}(t)]=0, \tag{28}$$

valid for any choice of vectors $\boldsymbol{u}$ and $\boldsymbol{v}$. Differentiating the two equations with respect to t at $t=0$, we obtain

$$M[\dot{\boldsymbol{F}},\boldsymbol{a}_0\otimes\boldsymbol{n}_0,\boldsymbol{a}_0\otimes\boldsymbol{u}]+L[\dot{\boldsymbol{a}}\otimes\boldsymbol{n}_0,\boldsymbol{a}_0\otimes\boldsymbol{u}]+L[\boldsymbol{a}_0\otimes\dot{\boldsymbol{n}},\boldsymbol{a}_0\otimes\boldsymbol{u}]+L[\boldsymbol{a}_0\otimes\boldsymbol{n}_0,\dot{\boldsymbol{a}}\otimes\boldsymbol{u}]=0$$

and

$$M[\dot{\boldsymbol{F}},\boldsymbol{a}_0\otimes\boldsymbol{n}_0,\boldsymbol{v}\otimes\boldsymbol{n}_0]+L[\dot{\boldsymbol{a}}\otimes\boldsymbol{n}_0,\boldsymbol{v}\otimes\boldsymbol{n}_0]+L[\boldsymbol{a}_0\otimes\dot{\boldsymbol{n}},\boldsymbol{v}\otimes\boldsymbol{n}_0]+L[\boldsymbol{a}_0\otimes\boldsymbol{n}_0,\boldsymbol{v}\otimes\dot{\boldsymbol{n}}]=0,$$

respectively. Finally, substituting $\boldsymbol{u}=\boldsymbol{n}_0$ or $\boldsymbol{v}=\boldsymbol{a}_0$, and taking Eqs. (27) and (28) into account, we obtain the relation $M[\dot{\boldsymbol{F}},\boldsymbol{a}_0\otimes\boldsymbol{n}_0,\boldsymbol{a}_0\otimes\boldsymbol{n}_0]=0$. Therefore, the normal to a generic point on the spinodal surface can be identified with the functional

$$\boldsymbol{N}_{\partial\mathcal{S}}(\boldsymbol{F}_0)=M[\boldsymbol{a}_0\otimes\boldsymbol{n}_0,\boldsymbol{a}_0\otimes\boldsymbol{n}_0,\_], \tag{29}$$

meaning that

$$M[\boldsymbol{a}_0\otimes\boldsymbol{n}_0,\boldsymbol{a}_0\otimes\boldsymbol{n}_0,\boldsymbol{T}]=0$$

for any tangent $\boldsymbol{T}$ to the spinodal. Comparing (26) and (29), we conclude that the normal to $\partial\mathcal{B}_{\mathcal{W}}$ at the coherent critical point $\boldsymbol{F}_*$ is always parallel to the normal to the spinodal at the same point. As a consequence, the only equations satisfied by a critical point are (20), (21), and (23), and therefore the two surfaces must touch, not at a single point, but along a codimension-2 surface in the phase space.

We conclude that in coherent thermodynamics, we should talk about a *critical set*, rather than a single critical point. The critical set is the set of stable solutions of the system (20), (21), and (23), which, generically, should be a subvariety of both the binodal and the spinodal of codimension 1 in each. More specifically, in 3D the coherent critical set, if it exists, is a set of dimension 7 in the nine-dimensional phase space, and in 2D it is a set of dimension 2 in the four-dimensional phase space. Since for isotropic solids the phase diagram can be drawn in the space of singular values of $\boldsymbol{F}$, it will exhibit the critical set as a point in 2D and as a line in 3D. Despite the relatively high dimensionality of the critical set (generically, it is not a point), its dimensional deficiency allows one to pass around it and reach continuously from one coherent phase to another.

For the elementary examples of coherent critical points, see [78,119]. In what follows, we discuss two nonelementary applications of the obtained formulas, showing that in superficially similar models of elastic solids, coherent critical sets may exist but may also be prohibited. The latter situation arises when either the system of Eqs. (20), (21), and (23) has no solutions, or when all of their solutions are unstable.

IV. GEOMETRICALLY NONLINEAR HADAMARD-FLORY SOLID

To illustrate the conditions of coherent criticality (20), (21), and (23), we now consider a very special isotropic energy density, which is the simplest generalization of the "elastic liquid" model, accounting for rigidity. Known as the Hadamard-Flory model, it is characterized by the energy density [30,36,120,121]

$$W(\boldsymbol{F})=h(\det\boldsymbol{F})+(\mu/2)|\boldsymbol{F}|^2. \tag{30}$$

The first term is the same double-well potential as in the "elastic liquid" model. It comes after adiabatic elimination of the composition variable from the Flory-Higgins energy of mixing of the solvent and the polymer. The second term in (30), containing the square of Frobenius norm of $\boldsymbol{F}$, is the Neo-Hookean elastic energy of the polymer network. The magnitude of this (shear-related) contribution to the energy is controlled by the rigidity modulus μ; in gels, its value is mostly affected by the degree of cross-linking. The frame-indifferent elastic energy (30) is obviously isotropic, as it can be rewritten in the form $W(\boldsymbol{F})=h(\sqrt{I_3})+(\mu/2)I_1$, where $I_1=\mathrm{Tr}\,\boldsymbol{C}$ and $I_3=\det\boldsymbol{C}$ are the standard orthogonal invariants, and we recall that $\boldsymbol{C}=\boldsymbol{F}^T\boldsymbol{F}$ is the objective Cauchy-Green strain tensor.

To provide some physical intuition regarding the nature of elastic instabilities potentially experienced by such solids, it is enough to mention that along the deformation paths $\boldsymbol{F}=\epsilon\boldsymbol{I}$, preserving isotropy, the conventional tangential bulk modulus

$$B=\frac{\mu}{3}+\frac{2\epsilon}{3}h'(d)+\epsilon d h''(d)$$

can soften (unless μ is very large). Moreover, the linear elastic longitudinal wave speed would disappear at the elastic æther threshold $B+(4/3)G=\mu+\epsilon d h''(d)=0$, where we used the fact that along the same deformation path the tangential shear modulus is

$$G=\frac{\mu}{2}-\frac{\epsilon}{2}h'(d).$$

A. Coherent binodal

We take advantage of a known fact [122] that to construct the surface of phase coexistence (the coherent binodal) for the Hadamard-Flory solid at sufficiently large values of μ, it is sufficient to consider simple laminates which are layered mixtures of two deformation gradients $\boldsymbol{F}_\pm$. The full set of equations that such a pair needs to satisfy is given by (15)–(18). These equations define the jump set for the Hadamard-Flory solid (30). Observe first that kinematic compatibility condition (15) implies

$$d_+=d_-(1+\boldsymbol{F}_-^{-T}\boldsymbol{n}\cdot\boldsymbol{a}),$$

where again $d_\pm=\det\boldsymbol{F}_\pm$. Using this equality, Eq. (15), and the formula for the Piola stress tensor,

$$\boldsymbol{P}=W_{\boldsymbol{F}}(\boldsymbol{F})=\mu\boldsymbol{F}+dh'(d)\boldsymbol{F}^{-T},$$

we can reduce the condition of traction continuity (16) to

$$\boldsymbol{a}=-([\![h']\!]d_-/\mu)\boldsymbol{F}_-^{-T}\boldsymbol{n}.$$

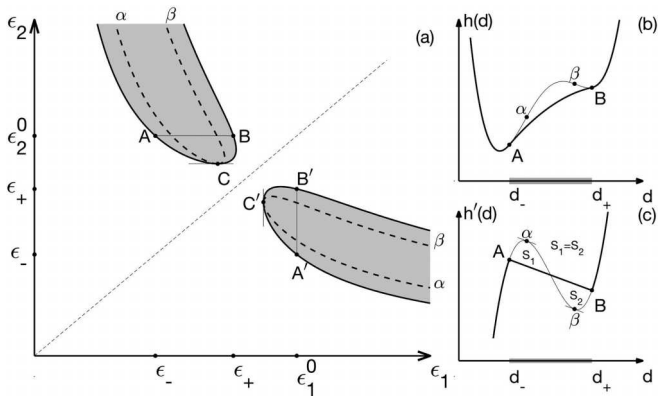

FIG. 2. (a) Phase diagram in the space of principal strains for a Hadamard-Flory solid with sufficiently large rigidity. (b) Double-well part of the energy along the line AB: $\epsilon_1 = d/\epsilon_2^0, \epsilon_2 = \epsilon_2^0$. (c) The corresponding pressure-volume relation along the line AB. The double-well part $\tilde{W}(\epsilon_1, \epsilon_2) - (\mu/2)(\epsilon_1^2 + \epsilon_2^2)$ of the relaxed (ground-state) energy and the relaxed stress-strain response are shown by solid lines. Binodal region in (a) is shaded. AB and $A'B'$ are typical pairs of coexisting states, C and C' are critical points. Dashed lines α, β enclose the spinodal region.

Then, using (17) we find that $\boldsymbol{n}$ must be an eigenvector of the Cauchy-Green strain tensor

$$\boldsymbol{C}_- = \boldsymbol{F}_-^T \boldsymbol{F}_-,$$

and also that $\boldsymbol{C}_+$ and $\boldsymbol{C}_-$ are related by

$$\boldsymbol{C}_+ = \boldsymbol{C}_- + (|\boldsymbol{a}|^2 - (2[\![h']\!]d_-/\mu))\boldsymbol{n} \otimes \boldsymbol{n}.$$

This implies that $\boldsymbol{C}_+$ and $\boldsymbol{C}_-$ are simultaneously diagonalizable. Therefore, there exist coordinate frames in both Lagrangian and Eulerian spaces in which both deformation gradients $\boldsymbol{F}_\pm$ are simultaneously diagonal, and they differ by a single eigenvalue $\epsilon_\pm$, corresponding to the eigenvector $\boldsymbol{n}$.

If we now denote the product of the remaining common eigenvalues of $\boldsymbol{F}_\pm$ (i.e., common singular values, in an arbitrary frame) by ϵ_0, then we can characterize the set of coexisting deformation gradients by the equation

$$\epsilon_0^2[\![h']\!] + \mu[\![d]\!] = 0, \tag{31}$$

where the relation between the values $d_\pm$ is found from (18), which now has the form

$$[\![h]\!] - \{h'\}[\![d]\!] = 0. \tag{32}$$

Note that Eqs. (31) and (32) can be interpreted geometrically as the equality of areas between the (tilted) line with the slope

$$[\![h']\!]/[\![d]\!] = -\mu/\epsilon_0^2 \tag{33}$$

and the graph of $h'(d)$; see Fig. 2(c). The nonzero slope in (33) implies that the classic (not "tilted") Maxwell common tangent construction no longer applies, and the relaxed energy, shown in Fig. 2(b), is no longer convex, due to the extensive mixing effects of purely elastic origin.

The foregoing analysis shows that we can draw a phase diagram in the two-dimensional plane, where one coordinate denotes one of the singular values of the deformation gradient $\boldsymbol{F}$, while the other denotes the product of the remaining ones. However, in 2D, both coordinates in such a phase diagram have the meaning of singular values of $\boldsymbol{F}$, making the interpretation of the figures more natural. Hence, one can view our figures as 2D phase diagrams in the space of singular values of $\boldsymbol{F}$, while keeping in mind that they can also be interpreted as phase diagrams in an arbitrary number of space dimensions. In the regime of sufficiently large μ, the set of coexisting states takes the form of two separate curves in the (ϵ_1, ϵ_2)-space, shown in Fig. 2(a). The presence of two symmetric subdomains $\epsilon_1 > \epsilon_2$ and $\epsilon_1 < \epsilon_2$ reflects the symmetry of the system with respect to the interchange of singular values of $\boldsymbol{F}$. In three space dimensions, the phase diagram would be represented by a single, say upper, curve, while the horizontal and vertical axes would be labeled as ϵ and ϵ_0, denoting one of the singular values of $\boldsymbol{F}$ and the product of the remaining ones, respectively. In what follows, our figures will always be drawn in the more intuitive 2D interpretation.

Note that our Fig. 2(a) should not be understood in the sense that the binodal region splits into a disjoint union of two components. In the actual four-dimensional phase space, the binodal region is connected. It looks like a four-dimensional torus, whose three-dimensional cross-section is the body of revolution of the shaded region, around the bisector of the first quadrant. Each point $\boldsymbol{F}_+$ on the binodal (the boundary of the binodal region) can coexist with a unique counterpart $\boldsymbol{F}_-$ on the binodal. Each pair $\boldsymbol{F}_\pm$ of such coexisting states is represented by two pairs of points (A, B) and (A', B') in our phase diagram Fig. 2(a).

More formally, viewed from the full 4D space of deformation gradients $\boldsymbol{F}$, these points represent traces of a 2D critical torus intersecting the subspace of diagonal matrices. Indeed, recall that a 2×2 matrix $\boldsymbol{F}$ can be written as $\boldsymbol{RDU}$, where $\{\boldsymbol{R}, \boldsymbol{U}\} \subset \mathrm{SO}(2)$, and $\boldsymbol{D}$ is diagonal with non-negative entries. If we represent each $\boldsymbol{F}$ by its diagonal form $\boldsymbol{D}$, then in the two-dimensional space of diagonal matrices each point corresponds to the entire $\mathrm{SO}(2) \times \mathrm{SO}(2) = S^1 \times S^1$ manifold in the $\boldsymbol{F}$-space. To express it more generally, each point in the n-dimensional space of singular values represents the $n(n-1)$-dimensional manifold $\mathrm{SO}(n) \times \mathrm{SO}(n)$; the critical set by itself is $(n^2 - 2)$-dimensional.

In striking contrast to what we have seen in the case of "elastic liquids," the binodal region does not partition the phase space into disjoint phases, and the values of $\boldsymbol{F}$ represented by the dashed line in Fig. 2(a) correspond to homogeneous (affine) configurations which remain globally stable, as one travels from the high-density phase to the lower. Even though the energy in this domain remains nonconvex, the equilibrium system does not form mixtures (microstructures) due to the prohibitively high rigidity-induced extensive cost of mixing.

Finally, we observe that the ensuing optimal microstructure is layered (simple laminate) with the layer normal being the common singular vector of $\boldsymbol{F}_\pm$ (eigenvector of $\boldsymbol{C}_\pm$) corresponding to singular values $\epsilon_\pm$. Since nonlinear elasticity is a scale-free theory, such microstructure does not have a scale and is represented only by the values $\boldsymbol{F}_\pm$ of deformation gradient in coexisting phases and the volume fraction controlled by the applied loading. More detailed information about the microstructure would be obtained in the models that incorporate an internal lengthscale which may be responsible, for instance, for surface tension.

B. Coherent spinodal

First recall that for the chosen material model, the acoustic tensor is

$$\boldsymbol{A}(\boldsymbol{n};\boldsymbol{F}) = \mu I + h''(d)\mathrm{cof}\boldsymbol{F}\boldsymbol{n} \otimes \mathrm{cof}\boldsymbol{F}\boldsymbol{n},$$

which makes it obvious that $\boldsymbol{A}(\boldsymbol{n};\boldsymbol{F})$ has only two distinct eigenvalues μ and $\mu + h''(d)|\mathrm{cof}\boldsymbol{F}\boldsymbol{n}|^2$. Adapting Eqs. (20) and (21) to this setting, we obtain

$$\mu\boldsymbol{a}_0 + h''(d)d^2(\boldsymbol{F}^{-1}\boldsymbol{a}_0 \cdot \boldsymbol{n}_0)\boldsymbol{F}^{-T}\boldsymbol{n}_0 = 0, \tag{34}$$

$$\mu\boldsymbol{n}_0 + h''(d)d^2(\boldsymbol{F}^{-1}\boldsymbol{a}_0 \cdot \boldsymbol{n}_0)\boldsymbol{F}^{-1}\boldsymbol{a}_0 = 0. \tag{35}$$

Eliminating unit vectors $\boldsymbol{n}_0$ and $\boldsymbol{a}_0$ from these equations, we obtain the characterization of the spinodal: $\boldsymbol{F} \in \partial\mathcal{S}$ if and only if

$$\mu\epsilon_{\min}^2 + d^2h''(d) = 0, \tag{36}$$

where we recall that $d = \det\boldsymbol{F}$, and $\epsilon_{\min}$ is the smallest singular value of $\boldsymbol{F}$. While Eq. (36), as well as other related equations obtained below, are valid in any number of space dimensions, we continue to illustrate them in two space dimensions. The spinodal, described by Eq. (36), is shown as a dashed line in Fig. 2(a). We see that the spinodal lies entirely inside the binodal region, except for the critical set represented in Fig. 2(a) by the points C and C'.

C. Coherent critical points

The exact location of the two (symmetry-related) critical points C and C' can be found as a solution of the system of Eqs. (20), (21), and (23). For the Hadamard-Flory solid, Eqs. (20) and (21) reduce to (36), while Eq. (23) becomes

$$h'''(d)d^3(\boldsymbol{F}^{-1}\boldsymbol{a}_0 \cdot \boldsymbol{n}_0)^3 = 0.$$

Taking a dot product of Eq. (35) with $\boldsymbol{n}_0$, we obtain $(\boldsymbol{F}^{-1}\boldsymbol{a}_0 \cdot \boldsymbol{n}_0)^2d^2h''(d) = -\mu$, which implies that $\boldsymbol{F}^{-1}\boldsymbol{a}_0 \cdot \boldsymbol{n}_0 \neq 0$. Thus, critical points solve the system of Eqs. (36), and

$$h'''(d) = 0. \tag{37}$$

For a typical double-well energy, we expect that Eq. (37) has a unique root d^*. The two singular values $\epsilon_1^* < \epsilon_2^*$ corresponding to the critical point are then given by

$$\epsilon_1^* = d^*\sqrt{-\frac{h''(d^*)}{\mu}}, \quad \epsilon_2^* = \frac{d^*}{\epsilon_1^*}.$$

This implies that unless $\mu > -d^*h''(d^*)$, there will be no critical points on the spinodal, i.e., the solution of (36) and (37) will lie in the interior of the spinodal region and will therefore be unstable. The critical point $(\epsilon_1^*, \epsilon_2^*)$ is shown as point C in Fig. 2(a). Point C', also shown in Fig. 2(a), is related to C by the coordinate interchange symmetry swapping ϵ_1 and ϵ_2.

We reiterate that according to our general theory, these points are located where the coherent spinodal and the coherent binodal touch each other in the phase space of deformation gradients $\boldsymbol{F}$. In this perspective, C and C' are not two different critical points and should be viewed instead as two visible (in our chosen section of the whole phase space) representatives of the critical set. More formally, in the n-dimensional space of singular values, the critical set will be represented by the $n^2 - 2 - n(n-1) = (n-2)$-dimensional submanifold. When $n = 2$, the critical set will be zero-dimensional, revealing itself in such a representation as a discrete set of points.

D. Ground-state energy

While it can be proved that the equilibrium (ground-state) energy $\tilde{W}(\boldsymbol{F})$ in the model with nonzero rigidity cannot be presented in the form $\tilde{h}(d) + \mu|\boldsymbol{F}|^2/2$, with $h(d)$ replaced by some new function $\tilde{h}(d)$ [122], the explicit formula for $\tilde{W}(\boldsymbol{F})$ can still be obtained in the large rigidity limit.

To explain the construction, we focus on one of the two symmetric regimes, and we set $\epsilon_1(\boldsymbol{F}) \leqslant \epsilon_2(\boldsymbol{F})$. We would also need to distinguish between the supercritical ($\epsilon_2 < \epsilon_2^*$) and subcritical ($\epsilon_2 > \epsilon_2^*$) cases.

Recall that since in the supercritical case mixing is suboptimal, we have

$$\tilde{W}(\epsilon_1, \epsilon_2) = W(\epsilon_1, \epsilon_2).$$

In the subcritical case, the expression for the equilibrium energy depends on whether the point $(\epsilon_1(\boldsymbol{F}), \epsilon_2(\boldsymbol{F}))$ is inside or outside the binodal region. Outside the binodal region, the homogeneous configurations are stable and we again have $\tilde{W}(\epsilon_1, \epsilon_2) = W(\epsilon_1, \epsilon_2)$. For the states inside the binodal region, the relaxed value of the energy can also be found since we know that there exists a uniquely determined pair of coexisting strains $\epsilon_-(\epsilon_2) < \epsilon_+(\epsilon_2)$, solving (31) and (32) with $\epsilon_0 = \epsilon_2$. Using these values, which represent parameters of energy-minimizing simple laminate, we can write an explicit expression for the relaxed energy inside the binodal region in the form

$$\tilde{W}(\epsilon_1, \epsilon_2) = \frac{\epsilon_1 - \epsilon_-}{\epsilon_+ - \epsilon_-}W(\epsilon_+, \epsilon_2) + \frac{\epsilon_+ - \epsilon_1}{\epsilon_+ - \epsilon_-}W(\epsilon_-, \epsilon_2).$$

Note that despite the simple mixture appearance of this formula, the relaxed energy is nonconvex. The reason is that the optimal simple laminate microstructure is prestressed due to the nontrivial interaction (nonadditivity) effects encoded in highly nonlinear Eqs. (31) and (32). Those interactions enter the relaxed energy implicitly via the nonlinear functions $\epsilon_\pm(\epsilon_2)$. This is manifested, for instance, by the failure of the conventional common tangent construction, which differs from the common area construction illustrated in Fig. 2(b). In other words, although the relaxed energy is a ruled surface, it is *flat* only in specific rank-1 directions while it still remains concave in some other non-rank-1 directions.

E. Stress space

To emphasize the nontrivial nature of the phase coexistence in the presence of nonzero rigidity, it is instructive to map the obtained phase diagram from the *strain* space into the *stress* space. This will allow us to characterize the same phase equilibria in the space of intensive variables akin to, say pressure and temperature, used in the classical thermodynamics. An experience with other systems exhibiting long-range interactions suggests that in such an "intensive" representation, the conventional *curves* representing "liquidlike" phase coexistence would transform into extended *domains* representing

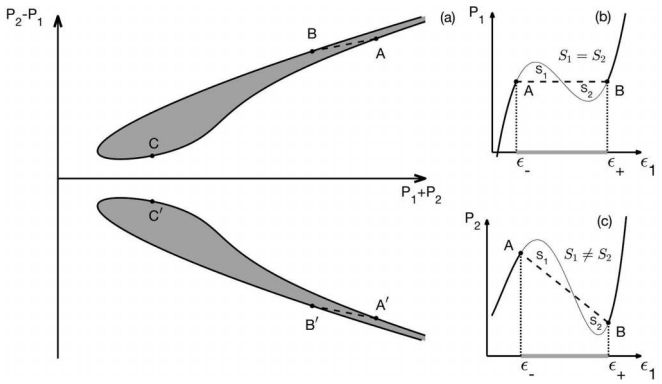

FIG. 3. (a) Phase diagram in the space of principal stresses for a Hadamard-Flory solid with sufficiently large rigidity. (b,c) Two stress-strain relations in a rank 1 loading direction (hard device); the stress-strain correspondence across the binodal region is shown by the dashed lines. Binodal region in (a) is shaded. The analogs of the graphs (b) and (c) for the pair of points A', B' are identical to them except the horizontal axes would be ϵ_2 and the labels P_1 and P_2 on the vertical axes would be interchanged.

"solidlike" phase coexistence [123,124]. As Fig. 3(a) shows, that is exactly what is happening.

To explain this figure, we first recall that in the coordinate frame where $\boldsymbol{F}$ is diagonal, the Piola stress $\boldsymbol{P}$ is also diagonal with components

$$P_{1,2} = \mu\epsilon_{1,2} + h'(\epsilon_1\epsilon_2)\epsilon_{2,1}. \tag{38}$$

The typical graphs of $P_1(\epsilon_1)$ and $P_2(\epsilon_1)$ at a given $\epsilon_2 = \epsilon_2^0$ are shown in Figs. 3(b) and 3(c). Note, in particular, that while the principal stresses P_1 are the same in the two coexisting phases A and B, the corresponding principal stresses P_2 in the same configurations are different.

Note also that, rather remarkably, the relation $P_2(\epsilon_1)$ does not satisfy the Maxwell equal area condition, which is nevertheless respected by the relation $P_1(\epsilon_1)$ along the same path AB in the strain space. This markedly different behavior is due to the tensorial (anisotropic) nature of stress in solids. Along the loading path AB, i.e., along the line segment joining $\boldsymbol{F}_+$ and $\boldsymbol{F}_-$ in the phase space, relations (16) and (18) are exactly the Maxwell relations we see operative in Fig. 3(b); other components of stress, like the one shown in Fig. 3(c), are not obligated by (16) and (18) to satisfy the Maxwell relations. We emphasize that, despite their apparent differences, Fig. 2(c) also illustrates exactly the same strain-stress relation. More specifically, along the path AB we have $d = \epsilon_1\epsilon_2^0$. Hence, the volumetric stress-strain response is effectively described by the function $P_1(\epsilon_1)$, and Fig. 2(c) simply shows the function $P_1(\epsilon_1) - \mu\epsilon_1$ in terms of d, while the graph of the function $P_1(\epsilon_1)$ is shown in Fig. 3(b). Note also that our Fig. 2(b) presents the double-well part $\tilde{W}(\boldsymbol{F}) - \mu|\boldsymbol{F}|^2/2$ of the relaxed energy. Subtracting from the relaxed energy density the quadratic term in the original energy transforms the Maxwell "common tangent line" into a "common tangent parabola" shown in Fig. 2(b) and changes the horizontal Maxwell line in Fig. 3(b) into a slanted Maxwell line in Fig. 2(c). In fact, one can show that our Fig. 3 illustrates a general phenomenon: the Maxwell property of the stress component $\boldsymbol{Pn} \cdot \boldsymbol{a}$.

The whole set of coexisting equilibrium stress components parametrized by ϵ_2^0, which is shown in Fig. 3(a), illustrates the relaxed response of our two-phase Hadamard-Flory solid. One can see the anticipated opening of a 2D coexistence domain in the space of intensive variables, which, as we have already mentioned, is typical for systems with long-range interactions [123]. In our case, such an opening is indicative of the presence of metastability and hysteresis in a soft loading device but not in a hard loading device; such an ensemble dependence of the equilibrium response is yet another characteristic property of systems with long-range interactions [123]. Other examples of the same effect can be found in [69,125] dealing with different types of elastic response.

Finally, note that the analysis of the AB path conducted above can be extended by symmetry to the $A'B'$ path also indicated in Fig. 3(a) inside the second symmetric coexistence domain parametrized by ϵ_1^0. [See also the second connected component of the binodal region in Fig. 2(a).] In particular, for the $A'B'$ path, the graphs of $P_{1,2}(\epsilon_2)$ (at a given $\epsilon_1 = \epsilon_1^0$) would be identical to the graphs of $P_{2,1}(\epsilon_1)$ (at a given $\epsilon_2 = \epsilon_2^0$) along the AB path shown in Figs. 3(b) and 3(c).

V. GEOMETRICALLY LINEAR HADAMARD-FLORY SOLID

Since the *geometrical nonlinearity* is usually neglected in problems involving bulk phases [126,127], it is natural to ask whether the rigidity-induced critical points survive in the model of the same solid but now relying exclusively on linear strains.

Observe first that there are no immediate mathematical reasons for a nonlinear energy, which depends on $\boldsymbol{F}$ only through a special combination

$$\boldsymbol{\epsilon} = (1/2)(\boldsymbol{F} + \boldsymbol{F}^T), \tag{39}$$

not to have stable critical points (where we only refer to purely volumetric, symmetry-preserving transformations). Note next that the assumptions that would formally justify geometric linearization would also automatically justify physical linearization, and then there would be no critical points; this last conclusion is vacuously true in the geometrically linearized theory of elastic phase transformations between two physically linear-elastic phases, since such an energy has no spinodal region.

In general, one cannot expect to find stable critical points often. This is because critical points are points of tangency between the binodal and the spinodal, and more often than not the spinodal lies entirely inside the binodal region. Even when such tangency does occur, stable critical points are in some sense the least stable points on the binodal. For this reason, any modification of the energy density function, making it easier to create energy-minimizing laminates, may destabilize parts of the binodal, in which case critical points might be the most vulnerable candidates for destabilization. This can already be seen from the fact that if one decreases the rigidity parameter μ in the Hadamard-Flory model (30), the rigidity-induced critical points eventually lose their stability.

We emphasize, though, that it is not the geometrical nonlinearity but the nonconvex physical nonlinearity of the energy

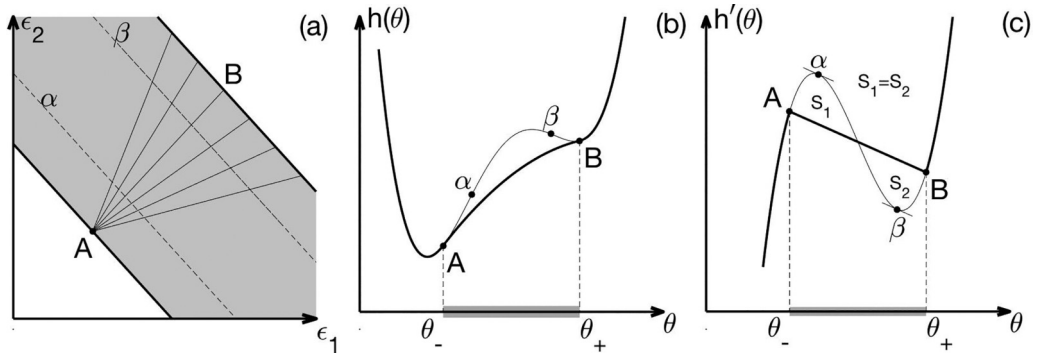

FIG. 4. (a) Phase diagram in the space of principal strains for a geometrically linear Hadamard solid. (b) Double-well part of the energy. (c) The corresponding stress-strain relation. The relaxed (ground-state) energy and the relaxed stress-strain response are shown by solid lines. Binodal region in (a) is shaded; dashed lines limit the spinodal region.

density in $\boldsymbol{F}$ that is the main cause of instability leading to phase transition. Replacing the energy density $\boldsymbol{F}$ by $\boldsymbol{\epsilon}$ from (39) formally retains exactly the same type of nonconvexity, however it makes the destabilization of a homogeneous state and the formation of laminates qualitatively easier, since the pair $\boldsymbol{F}_\pm$ is compatible if $[\![\boldsymbol{F}]\!]$ is rank 1, while the pair $\boldsymbol{\epsilon}_\pm$ is compatible if $[\![\boldsymbol{\epsilon}]\!]$ is rank 2, and some additional inequalities are satisfied. This means that the compatibility set of $\boldsymbol{\epsilon}_\pm$ has higher dimensionality than the compatibility set of $\boldsymbol{F}_\pm$, which may in principle contribute to the destabilization of the "bridge" between the stable components of the coherent binodal, which we have seen forming in the Hadamard-Flory solid in the limit of sufficiently strong rigidity. Since the presence of such a "bridge" is the factor allowing the two phases to be smoothly connected, the stable critical points would then disappear as well.

As follows from this discussion, the fate of coherent critical points under geometric linearization is not clear in the general case. However, as we show below, the rigidity-induced coherent critical points do completely disappear if we replace our geometrically nonlinear Hadamard-Flory solid by its geometrically (but not physically) linear version. In other words, critical points disappear if we consider a solid of Hadamard-Flory type, similarly undergoing a purely volumetric phase transition, but now with a geometrically linear but physically nonlinear elastic response in each of the phases. This example can then be used as an illustration of the utmost importance of a geometrically exact description of elastic deformation in soft solids.

In view of the approximation

$$\det \boldsymbol{F} \approx 1 + \mathrm{Tr}(\boldsymbol{F} - \boldsymbol{I}),$$

which is valid in the limit $\boldsymbol{F} \to \boldsymbol{I}$, the natural geometrically linear analog of the Hadamard-Flory energy density is

$$W(\boldsymbol{F}) = h(\mathrm{Tr}\boldsymbol{\epsilon}) + \mu|\boldsymbol{\epsilon}|^2, \tag{40}$$

where $\boldsymbol{\epsilon}$ is defined in (39). Note that the geometrically linear version (40) of the Hadamard-Flory solid is significantly less nonlinear than the original one. For example, for the double-well potential h, the geometrically nonlinear energy (30) is not rank-1 convex, no matter how large $\mu > 0$ is. By contrast, energy (40) will become convex when μ is sufficiently large, assuming the double-well potential h is smooth.

A. Coherent binodal

It is natural to start again with the characterization of the geometrically linearized jump set, i.e., the set of equilibrium coexisting strain tensors $\boldsymbol{\epsilon}$. Using the kinematic compatibility condition (15), which now takes the form

$$[\![\boldsymbol{\epsilon}]\!] = (1/2)(\boldsymbol{a} \otimes \boldsymbol{n} + \boldsymbol{n} \otimes \boldsymbol{a}),$$

and the linearized analog of the traction continuity condition (16)

$$([\![h'(\mathrm{Tr}\boldsymbol{\epsilon})]\!]\boldsymbol{I} + 2\mu[\![\boldsymbol{\epsilon}]\!])\boldsymbol{n} = 0, \tag{41}$$

we obtain $\boldsymbol{a} = \lambda \boldsymbol{n}$. Substituting $\boldsymbol{a} = \lambda \boldsymbol{n}$ back into (41), we obtain

$$\lambda = -[\![h']\!]/2\mu. \tag{42}$$

The analog of condition (17) is now satisfied automatically, since in geometrically linear elasticity the Piola stress tensor is symmetric, and since for the linearized Hadamard-Flory solid, $\boldsymbol{a}$ is a scalar multiple of $\boldsymbol{n}$.

Finally, in the linearized theory, condition (18) (generalized Maxwell relation) takes the form

$$[\![h]\!] - \{h'\}[\![\theta]\!] = 0,$$

where $\theta = \mathrm{Tr}\,\boldsymbol{\epsilon}$. This, together with (42), means geometrically that $\theta_- = \mathrm{Tr}\,\boldsymbol{\epsilon}_-$ and $\theta_+ = \mathrm{Tr}\,\boldsymbol{\epsilon}_+$ are the two points of common tangency to the graph of $h(\theta) + \mu\theta^2$. Note, however, that, unless $\mu = 0$, this construction still differs from the conventional Maxwell (common tangent) construction for the volumetric part of the energy $h(\theta)$; see Figs. 4(b) and 4(c). Therefore, the binodal region in the space (ϵ_1, ϵ_2) of the eigenvalues of the linearized strain tensor $\boldsymbol{\epsilon}$ is delimited by straight lines,

$$\mathrm{Tr}\boldsymbol{\epsilon} = \theta_\pm,$$

see Fig. 4(a). Moreover, similar to the "liquid" case and in contrast with the nonlinear "solid" case, the optimal laminates in the geometrically linearized Hadamard-Flory theory are not unique. We illustrate this effect in Fig. 4(a) by indicating schematically infinitely many admissible rank-1 connections between the state A and different states B. It is also interesting that, in contradistinction with the geometrically exact theory, at large values of μ, the linearized binodal region may completely disappear as the energy becomes convex.

It is important to mention that, in contrast to what we had in geometrically nonlinear theory, here the morphology of nucleating precipitates in the infinite domain can be completely arbitrary, like in a liquid [77]. In particular, for example, the microstructure may be represented by simple laminates, as in geometrically nonlinear theory, but now with an arbitrarily chosen orientation of layers. In view of the fact that the equilibrium configurations do not satisfy our basic nondegeneracy condition $\boldsymbol{H} > 0$, the geometrically linear theory in this example exhibits extreme morphological nonuniqueness. For instance, in any homogeneously strained finite domain, Hashin's concentric sphere construction [128] delivers infinitely many different (but energetically equivalent) minimizers with fractal phase boundaries; the existence of such scale-free minimizers is a general feature of elasticity theory, where the energy density depends only on $\nabla \boldsymbol{y}$.

B. Ground-state energy

In this example, we can also compute the relaxed (ground-state) energy explicitly, which can now be written in the form [79]

$$\tilde{W}(\boldsymbol{\epsilon}) = \tilde{h}(\mathrm{Tr}\,\boldsymbol{\epsilon}) + \mu|\boldsymbol{\epsilon}|^2.$$

Inside the binodal region, which is the domain of phase coexistence, $\theta_- < \mathrm{Tr}\,\boldsymbol{\epsilon} < \theta_+$, we find that

$$\tilde{h}(\theta) = \{h'\}(\theta - \{\theta\}) + \{h\} + \mu(\theta - \theta_-)(\theta_+ - \theta), \quad (43)$$

while $\tilde{h}(\theta) = h(\theta)$ outside. Formula (43) can be easily derived from the general relaxation formula [[81], Lemma 4.3]

$$\widetilde{W}(\boldsymbol{F}) = \tau W(\boldsymbol{F}_+) + (1-\tau)W(\boldsymbol{F}_-),$$

provided $\boldsymbol{F} = \tau\boldsymbol{F}_+ + (1-\tau)\boldsymbol{F}_-$ for some $\tau \in (0,1)$, where $\boldsymbol{F}_+$ and $\boldsymbol{F}_-$ are stable, rank-1 related, and satisfy the so called normality condition $\mathrm{Tr}\,([\![\boldsymbol{P}]\!]^T[\![\boldsymbol{F}]\!]) = 0$. Note that the laminate construction behind formula (43) produces relaxed nonlinear potential $\tilde{h}$, which is different from the straightforward convexification of $h(\theta)$, because of the persistent extensive mixing effects; see Fig. 4(b).

C. Coherent spinodal

In the geometrically linearized theory, the equations of spinodal (20) and (21) reduce to

$$h''(\theta) = -2\mu. \quad (44)$$

According to Eq. (42),

$$[\![\theta]\!] = \mathrm{Tr}\,([\![\boldsymbol{\epsilon}]\!]) = \boldsymbol{a}\cdot\boldsymbol{n} = \lambda = -\frac{[\![h']\!]}{2\mu}.$$

Applying the Lagrange theorem, we conclude that at least one solution of (44) must be in the interval (θ_-, θ_+). In fact, for double-well potentials $h(\theta)$, Eq. (44) has exactly two solutions α and β, shown by dashed lines in Fig. 4(a) and also marked in Figs. 4(b) and 4(c). As is evident from Fig. 4(a), the spinodal never touches the binodal.

D. Coherent critical points

In the geometrically linearized setting, the tensorial Eq. (23), defining the rigidity-induced critical points, turns into

$$h'''(\theta) = 0. \quad (45)$$

The two Eqs. (44) and (45) for a single unknown θ are generically incompatible. When they are compatible (say, at a special value of μ for a given h), the binodal region in Fig. 4(a) collapses to a line, coinciding with the similarly collapsed spinodal region. For all other values of μ, the critical points are absent. To summarize, if the geometrically exact model of a solid is replaced by the simplified geometrically linearized description, rigidity-induced coherent critical points may completely disappear. This result highlights, for instance, the crucial importance of a geometrically exact description of elastic deformation in living cells and tissues where the necessity for the appropriate reformulation of the early geometrically linear approaches has long been realized [10,129–133].

VI. CONCLUSIONS

In this paper, we studied the role of finite elastic rigidity in diffusionless solid-solid first-order phase transitions. Relying on the developed methods of coherent thermodynamics of elastic solids, we corroborated the general claim that the rigorous incorporation of rigidity into thermodynamic theory of phase transitions can lead not only to quantitative but also to qualitative effects.

We focused on the question of the possible existence, in the coherent (or kinetic) phase diagrams, of an unconventional type of rigidity-induced "coherent critical points," which are fundamentally different from the conventional critical points encountered in rigidity-free (liquid) systems. To answer this question, we had to systematically develop a general theory of such critical points in physically and geometrically nonlinear elastic solids. In particular, we presented the complete set of explicit equations, allowing one to locate "coherent critical points" in the space of deformation gradients.

Our analysis relies on the assumption (of kinetic origin) that elasticity is an equilibrium property of solids. It implies strain compatibility, which prevents atoms from exchanging places, and ultimately brings into continuum theory effective long-range interactions. Taking such elastic long-range interactions into consideration requires geometrically exact description of nonhydrostatic deformation, which, for instance, destroys the additivity of the energy, producing extensive mixing effects, and making the energy of a phase mixture sensitive not only to volume fractions of the coexisting phases, as is the case in liquid systems, but also to the geometrical details of two-phase microstructures. This violates one of the foundations of the Gibbsian thermodynamics of phase transformations and expectedly brings about significant implications.

To demonstrate that the emergence of the new type of critical points is one of the rigidity-induced *qualitative* effects, we systematically studied the loss of stability of a homogeneous state, when the deformation gradient crosses into the coherent binodal region. In this case, the knowledge of the geometry of emerging energy-minimizing two-phase configurations is crucial for the determination of stability limits. Along the way,

one needs to fully characterize the set of pairs of deformation gradients that could coexist at the coherent phase boundary.

We showed that if the complement of the coherent binodal region in the space of deformation gradient is connected, which requires that the corresponding energy wells are not geometrically compatible, there exists a possibility to pass from one phase to another without the actual sharp phase transformation. The existence of such passages implies the presence of rigidity-induced critical points, whose detailed quantitative characterization in the framework of nonlinear elasticity constitutes the main result of the paper.

To illustrate the obtained general results, we applied the developed theory to the description of a zero-temperature equilibrium response of an isotropic solid undergoing a purely volumetric, first-order phase transition. Similar transformations in liquid systems, such as liquid-gas phase transitions, usually exhibit critical points in the pressure-temperature space, which is a natural consequence of the fact that phases have the same symmetry and can, in principle, be continuously transformed into one another. To eliminate this type of (classical thermodynamic) criticality, we have chosen our parameters in such a way that the conventional critical points do not exist.

We then showed that when rigidity is sufficiently large, the entire set of coexisting phases is stable, ensuring that specially oriented simple laminates are sufficient to characterize the ground-state energy. We further observed that in the regime of interest, the complement of the coherent binodal region is indeed connected. As we have already mentioned, this signals the emergence of the new type of nonclassical (coherent) critical points.

Around such points, which we can locate by examining the stability of solutions of our fundamental system of algebraic Eqs. (20), (21), and (23), one can expect anomalous fluctuations and the critical opalescence, which have indeed been observed in swelling gels [13,23,31]. The corresponding "coherent" scaling relations remain to be determined. The crucial insight here may be that phase nucleation in coherent systems involves the configurational "delocalization" in the strain space which can interfere with the conventional real-space divergence of the correlation length.

To emphasize that the geometrically exact modeling of a solid was absolutely essential for capturing the coherent critical points in our example, we considered it in juxtaposition with a standard description of the same volumetric phase transition within the framework of linearized kinematics. Perhaps unexpectedly for many, we discovered that in this, more broadly accepted setting of elasticity theory, the rigidity-induced coherent critical points disappear. This discovery highlights the importance of not only physical, but also geometrical nonlinearity, which is necessary for the accurate accounting of elastic effects in highly deformable solids. In this sense, our study can be viewed as a cautionary tale, stressing the importance of finite strains in the thermodynamic description of phase transitions in soft matter.

Finally, we mention that the applicability of our results is not limited to volumetric phase transitions in isotropic gels, even though we used the well-studied swelling transitions in gels as our main example. Instead, our approach is sufficiently general to be used for the description of arbitrary anisotropic nonlinear elastic solids undergoing first-order phase transitions with arbitrary transformation strains. In this sense, our results can be expected to have implications in a broader range of research fields, from living matter to artificial biomimetic metamaterials, exhibiting symmetry-preserving phase transitions.

ACKNOWLEDGMENTS

Y.G. was supported by the National Science Foundation under Grant No. DMS-2305832. L.T. was supported by the French Grant No. ANR-10-IDEX-0001-02 PSL.

[1] J. W. Cahn, Acta Metall. **10**, 907 (1962).
[2] R. O. Williams, Metall. Trans. A **11**, 247 (1980).
[3] V. Kuznetsov, P. Moskvin, and V. Sorokin, J. Cryst. Growth **88**, 241 (1988).
[4] D. M. Wood and A. Zunger, Phys. Rev. B **40**, 4062 (1989).
[5] I. A. Abrikosov, A. Knutsson, B. Alling, F. Tasnádi, H. Lind, L. Hultman, and M. Odén, Materials **4**, 1599 (2011).
[6] D. A. Cogswell and M. Z. Bazant, ACS Nano **6**, 2215 (2012).
[7] M. G. Forest, Q. Wang, and R. Zhou, Rheol. Acta **43**, 17 (2004).
[8] P. Maugis, Comput. Mater. Sci. **159**, 460 (2019).
[9] P. Maugis, J. Phase Equilib. Diff. **43**, 827 (2022).
[10] J. Little, A. J. Levine, A. R. Singh, and R. Bruinsma, Phys. Rev. E **107**, 024418 (2023).
[11] A. G. Khachaturyan, *Theory of Structural Transformation in Solids* (Wiley, New York, 1983).
[12] K. Bhattacharya, *Microstructure of martensite. Why it forms and how it gives rise to the shape-memory effect*, Oxford Series on Materials Modelling, Vol. 2 (Oxford University Press, Oxford, 2003).
[13] Y. Li and T. Tanaka, Annu. Rev. Mater. Sci. **22**, 243 (1992).
[14] A. Onuki, in *Responsive Gels: Volume Transitions I*, Advances in Polymer Science Vol. 109, edited by K. Dušek (Springer, Berlin, 1993), pp. 63–121.
[15] B. Yan, H. Zhou, J. Lai, Z. Wang, C. Luo, H. Liu, X. Jin, A. Ma, and W. Chen, Polym. Bull. **76**, 6049 (2019).
[16] M. S. Dimitriyev, Y.-W. Chang, P. M. Goldbart, and A. Fernández-Nieves, Nano Futures **3**, 042001 (2019).
[17] T. Tanaka, Physica A **140**, 261 (1986).
[18] T. Hwa and M. Kardar, Phys. Rev. Lett. **61**, 106 (1988).
[19] K. Sekimoto and K. Kawasaki, J. Phys. Soc. Jpn. **57**, 2594 (1988).
[20] E. Sato Matsuo and T. Tanaka, J. Chem. Phys. **89**, 1695 (1988).
[21] E. S. Matsuo and T. Tanaka, Nature (London) **358**, 482 (1992).
[22] D. Ruelle, *Statistical Mechanics* (Benjamin, New York, 1969).
[23] T. Tanaka, D. Fillmore, S.-T. Sun, I. Nishio, G. Swislow, and A. Shah, Phys. Rev. Lett. **45**, 1636 (1980).
[24] K. Sekimoto, N. Suematsu, and K. Kawasaki, Phys. Rev. A **39**, 4912 (1989).

[25] A. Onuki, Phys. Rev. A **38**, 2192 (1988).
[26] T. Tanaka, S. Ishiwata, and C. Ishimoto, Phys. Rev. Lett. **38**, 771 (1977).
[27] R. Lakes and K. Wojciechowski, Phys. Status Solidi B **245**, 545 (2008).
[28] A. Larkin and S. Pikin, Sov. Phys. JETP **29**, 891 (1969).
[29] L. Golubović and T. C. Lubensky, Phys. Rev. Lett. **63**, 1082 (1989).
[30] P. J. Flory, *Principles of Polymer Chemistry* (Cornell University Press, Ithaca, NY, 1953).
[31] T. Tanaka, Phys. Rev. Lett. **40**, 820 (1978).
[32] K. Sekimoto and K. Kawasaki, J. Phys. Soc. Jpn. **56**, 2997 (1987).
[33] A. Onuki, J. Phys. Soc. Jpn. **57**, 703 (1988).
[34] K. Sekimoto and K. Kawasaki, Physica A **154**, 384 (1989).
[35] A. Onuki, Phys. Rev. A **39**, 5932 (1989).
[36] N. Suematsu, K. Sekimoto, and K. Kawasaki, Phys. Rev. A **41**, 5751 (1990).
[37] S. Panyukov and Y. Rabin, Macromolecules **29**, 7960 (1996).
[38] B. Barrière, K. Sekimoto, and L. Leibler, J. Chem. Phys. **105**, 1735 (1996).
[39] J.-i. Maskawa, T. Takeuchi, K. Maki, K. Tsujii, and T. Tanaka, J. Chem. Phys. **110**, 10993 (1999).
[40] F. Larché and J. W. Cahn, Acta Metall. **21**, 1051 (1973).
[41] F. Larche and J. Cahn, Acta Metall. **26**, 1579 (1978).
[42] O. Penrose, Markov Proc. Relat. Fields **8**, 351 (2002).
[43] S. R. Williams and D. J. Evans, J. Chem. Phys. **131**, 024115 (2009).
[44] S. R. Williams and D. J. Evans, J. Chem. Phys. **132**, 184105 (2010).
[45] S. R. Williams, J. Chem. Phys. **135**, 131102 (2011).
[46] R. Kotecký and S. Luckhaus, Commun. Math. Phys. **326**, 887 (2014).
[47] S. Saw and P. Harrowell, Phys. Rev. Lett. **116**, 137801 (2016).
[48] P. Nath, S. Ganguly, J. Horbach, P. Sollich, S. Karmakar, and S. Sengupta, Proc. Natl. Acad. Sci. USA **115**, E4322 (2018).
[49] F. Sausset, G. Biroli, and J. Kurchan, J. Stat. Phys. **140**, 718 (2010).
[50] P. Podio-Guidugli, J. Elast. **58**, 1 (2000).
[51] A. E. Green and W. Zerna, *Theoretical Elasticity* (Dover, New York, 1992).
[52] R. Ogden, *Non-Linear Elastic Deformations* (Dover, Mineola, New York, 1997).
[53] A. I. Lurie, *Non-Linear Theory of Elasticity* (North-Holland, Amsterdam, 1990).
[54] J. J. Stoker, *Nonlinear Elasticity* (Gordon and Breach Science Publishers, New York, 1968).
[55] P. G. Ciarlet, *Mathematical Elasticity: Three-dimensional Elasticity* (SIAM, Philadelphia, 2022).
[56] E. Agoritsas, R. García-García, V. Lecomte, L. Truskinovsky, and D. Vandembroucq, J. Stat. Phys. **164**, 1394 (2016).
[57] Y. Pomeau, C. R. Mec. **330**, 249 (2002).
[58] D. Bonn, M. M. Denn, L. Berthier, T. Divoux, and S. Manneville, Rev. Mod. Phys. **89**, 035005 (2017).
[59] M. E. Gurtin, E. Fried, and L. Anand, *The Mechanics and Thermodynamics of Continua* (Cambridge University Press, Cambridge, UK, 2010).
[60] M. Silhavy, *The Mechanics and Thermodynamics of Continuous Media* (Springer-Verlag, Berlin, 1997).
[61] M. Kružík and T. Roubíček, *Mathematical Methods in Continuum Mechanics of Solids* (Springer, Cham, Switzerland, 2019).
[62] J. W. Cahn and F. Larché, Acta Metall. Mater. **32**, 1915 (1984).
[63] A. Roitburd, Sov. Phys. Solid State **26**, 1229 (1984).
[64] W. C. Johnson and P. Voorhees, Metall. Trans. A **18**, 1213 (1987).
[65] J. Sak, Phys. Rev. B **10**, 3957 (1974).
[66] R. B. Schwarz and A. G. Khachaturyan, Phys. Rev. Lett. **74**, 2523 (1995).
[67] R. Schwarz and A. Khachaturyan, Acta Mater. **54**, 313 (2006).
[68] R. V. Kohn, Contin. Mech. Thermodyn. **3**, 193 (1991).
[69] J. Ball and R. James, Arch. Ration. Mech. Anal. **218**, 1363 (2015).
[70] Y. M. Jin, Y. U. Wang, and A. G. Khachaturyan, Acta Mater. **173**, 292 (2019).
[71] R. Williams, Calphad **8**, 1 (1984).
[72] W. C. Johnson, Metall. Mater. Trans. A **18**, 1093 (1987).
[73] C. B. Morrey, Pacific J. Math. **2**, 25 (1952).
[74] J. M. Ball, Arch. Ration. Mech. Anal. **63**, 337 (1976).
[75] B. Dacorogna, J. Funct. Anal. **46**, 102 (1982).
[76] J. L. Ericksen and R. A. Toupin, Can. J. Math. **8**, 432 (1956).
[77] Y. Grabovsky and L. Truskinovsky, J. Nonlin. Sci. **23**, 891 (2013).
[78] G. Fadda, L. Truskinovsky, and G. Zanzotto, Phys. Rev. B **68**, 134106 (2003).
[79] Y. Grabovsky and L. Truskinovsky, J. Nonlin. Sci. **29**, 229 (2019).
[80] Y. Grabovsky and L. Truskinovsky, Arch. Ration. Mech. Anal. **200**, 183 (2011).
[81] Y. Grabovsky and L. Truskinovsky, J. Nonlin. Sci. **24**, 1125 (2014).
[82] C. J. Gagne, H. Gould, W. Klein, T. Lookman, and A. Saxena, Phys. Rev. Lett. **95**, 095701 (2005).
[83] D. W. Herrmann, W. Klein, and D. Stauffer, Phys. Rev. Lett. **49**, 1262 (1982).
[84] L. D. Landau and E. M. Lifshitz, *Statistical Physics: Part 1*, Course of Theoretical Physics, Vol. 5 (Elsevier, Amsterdam, 1980).
[85] B. Dacorogna, Arch. Rational Mech. Anal. **77**, 359 (1981).
[86] J. L. Ericksen, J. Elasticity **5**, 191 (1975).
[87] K. Aizu, J. Phys. Soc. Jpn. **27**, 387 (1969).
[88] T. Lookman, S. R. Shenoy, K. O. Rasmussen, A. Saxena, and A. R. Bishop, Phys. Rev. B **67**, 024114 (2003).
[89] R. Vasseur and T. Lookman, Phys. Rev. B **81**, 094107 (2010).
[90] E. K. Salje, Annu. Rev. Mater. Res. **42**, 265 (2012).
[91] E. J. McShane, Ann. Math. **32**, 578 (1931).
[92] L. M. Graves, Duke Math. J. **5**, 656 (1939).
[93] J. Dunn and R. Fosdick, J. Elasticity **34**, 167 (1994).
[94] M. Guymont, Phys. Rev. B **24**, 2647 (1981).
[95] J. Sapriel, Phys. Rev. B **12**, 5128 (1975).
[96] J. D. Eshelby, in *Inelastic Behavior of Solids*, edited by M. F. Kanninen, W. F. Adler, A. R. Rosenfeld, and R. I. Jaffee (McGraw-Hill, New York, 1970), pp. 77–114.
[97] G. Erdmann, J. Reine Angew. Math. **82**, 21 (1877).
[98] I. M. Gelfand and S. V. Fomin, *Calculus of Variations* (Dover Publications, 2000).
[99] K. A. Lurie, *Applied Optimal Control Theory of Distributed Systems*, Mathematical Concepts and Methods in Science and Engineerings, Vol. 43 (Plenum, New York, 1993).

[100] A. Cherkaev, *Variational Methods for Structural Optimization*, Applied Mathematical Sciences, Vol. 140 (Springer-Verlag, New York, 2000).
[101] G. Allaire, *Shape Optimization by the Homogenization Method*, Applied Mathematical Sciences, Vol. 146 (Springer-Verlag, New York, 2001).
[102] P.-Y. F. Robin, Am. Mineral. **59**, 1286 (1974).
[103] J. K. Knowles, J. Elasticity **9**, 131 (1979).
[104] R. D. James, Arch. Ration. Mech. Anal. **77**, 143 (1981).
[105] R. L. Fosdick and G. MacSithigh, Arch. Rational Mech. Anal. **84**, 31 (1983).
[106] M. E. Gurtin, Arch. Ration. Mech. Anal. **84**, 1 (1983).
[107] M. Grinfeld, Sov. Phys. Dokl. **31**, 831 (1986).
[108] P. Rosakis, J. Mech. Phys. Solids **40**, 1163 (1992).
[109] E. Fried, J. Elasticity **31**, 71 (1993).
[110] A. B. Freidin, Z. Angew. Math. Mech. **87**, 102 (2007).
[111] K. A. Lurie, Prikl. Mat. Mekh. **34**, 270 (1970).
[112] A. L. Roitburd and N. S. Kosenko, Phys. Status Solidi A **35**, 735 (1976).
[113] L. B. Kublanov and A. B. Freidin, Prikl. Mat. Mekh. **52**, 493 (1988).
[114] S. A. Silling, J. Elasticity **19**, 241 (1988).
[115] A. Roytburd and J. Slutsker, J. Mech. Phys. Solids **49**, 1795 (2001).
[116] M. Šilhavý, in *Mechanics of Material Forces*, Advances in Mechanics and Mathematics, Vol. 11 (Springer, New York, 2005), pp. 281–288.
[117] V. I. Levitas, I. B. Ozsoy, and D. L. Preston, Europhys. Lett. **78**, 16003 (2007).
[118] B. Dacorogna, *Direct Methods in the Calculus of Variations*, 2nd ed. (Springer-Verlag, New York, 2008).
[119] B. Budiansky and L. Truskinovsky, J. Mech. Phys. Solids **41**, 1445 (1993).
[120] J. Hadamard, *Leçons sur la Propagation des Ondes et les Equations de l'Hydrodynamique* (Hermann, Paris, 1903).
[121] A. Onuki, J. Phys. Soc. Jpn. **57**, 699 (1988).
[122] Y. Grabovsky and L. Truskinovsky, J. Elasticity **135**, 351 (2019).
[123] S. Gupta and S. Ruffo, Int. J. Mod. Phys. A **32**, 1741018 (2017).
[124] A. Campa, T. Dauxois, and S. Ruffo, Phys. Rep. **480**, 57 (2009).
[125] Y. Grabovsky and L. Truskinovsky, J. Elasticity **154**, 147 (2023).
[126] L. D. Landau, E. M. Lifshitz, *Theory of Elasticity*, Course of Theoretical Physics, Vol. 7 (Butterworth-Heinemann, Oxford, UK, 1986).
[127] P. M. Chaikin and T. C. Lubensky, *Principles of Condensed Matter Physics* (Cambridge University Press, Cambridge, 1995).
[128] Z. Hashin, ASME J. Appl. Mech. **29**, 143 (1962).
[129] Y. Shokef and S. A. Safran, Phys. Rev. Lett. **108**, 178103 (2012).
[130] P. Nardinocchi, L. Teresi, and V. Varano, Int. J. Nonlin. Mech. **56**, 34 (2013).
[131] J. Feng, H. Levine, X. Mao, and L. M. Sander, Soft Matter **12**, 1419 (2016).
[132] O. Szachter, E. Katzav, M. Adda-Bedia, and M. Moshe, Phys. Rev. E **107**, 045002 (2023).
[133] G. Grekas, M. Proestaki, P. Rosakis, J. Notbohm, C. Makridakis, and G. Ravichandran, J. R. Soc. Interface **18**, 20200823 (2021).